

**Contract No:**

This document was prepared in conjunction with work accomplished under Contract No. DE-AC09-08SR22470 with the U.S. Department of Energy (DOE) Office of Environmental Management (EM).

**Disclaimer:**

This work was prepared under an agreement with and funded by the U.S. Government. Neither the U. S. Government or its employees, nor any of its contractors, subcontractors or their employees, makes any express or implied:

- 1 ) warranty or assumes any legal liability for the accuracy, completeness, or for the use or results of such use of any information, product, or process disclosed; or
- 2 ) representation that such use or results of such use would not infringe privately owned rights; or
- 3) endorsement or recommendation of any specifically identified commercial product, process, or service.

Any views and opinions of authors expressed in this work do not necessarily state or reflect those of the United States Government, or its contractors, or subcontractors.



Savannah River  
National Laboratory®

A U.S. DEPARTMENT OF ENERGY NATIONAL LABORATORY • SAVANNAH RIVER SITE • AIKEN, SC

# **Modeling the Destruction of Glycolate in the Defense Waste Processing Facility (DWPF) Recycle Stream and Concentration Factors for Glycolate in the 2H Evaporator**

**M. J. Siegfried**

**S. P. Harris**

**C. A. Nash**

**W. H. Woodham**

**T. L. White**

September 2020

SRNL-STI-2020-00247, Revision 0

SRNL.DOE.GOV

## **DISCLAIMER**

This work was prepared under an agreement with and funded by the U.S. Government. Neither the U.S. Government or its employees, nor any of its contractors, subcontractors or their employees, makes any express or implied:

1. warranty or assumes any legal liability for the accuracy, completeness, or for the use or results of such use of any information, product, or process disclosed; or
2. representation that such use or results of such use would not infringe privately owned rights; or
3. endorsement or recommendation of any specifically identified commercial product, process, or service.

Any views and opinions of authors expressed in this work do not necessarily state or reflect those of the United States Government, or its contractors, or subcontractors.

**Printed in the United States of America**

**Prepared for  
U.S. Department of Energy**

**Keywords:** *Glycolate Thermolysis*  
*Glycolate Destruction*  
*Nitric-Glycolic Flowsheet*

**Retention:** *Permanent*

# **Modeling the Destruction of Glycolate in the Defense Waste Processing Facility (DWPF) Recycle Stream and Concentration Factors for Glycolate in the 2H Evaporator**

M. J. Siegfried  
S. P. Harris  
C. A. Nash  
W. H. Woodham  
T. L. White

September 2020

---

Prepared for the U.S. Department of Energy under contract number DE-AC09-08SR22470.



OPERATED BY SAVANNAH RIVER NUCLEAR SOLUTIONS

## REVIEWS AND APPROVALS

### AUTHORS:

---

M. J. Siegfried, Chemical Flowsheet Development Date

---

S. P. Harris, Advanced Modeling, Simulation and Analytics Date

---

C. A. Nash, Separation Sciences and Engineering Date

---

W. H. Woodham, Chemical Flowsheet Development Date

---

T. L. White, Spectroscopy, Separations and Log Date

### TECHNICAL REVIEW:

---

D. P. Lambert, Chemical Flowsheet Development Date

---

J. E. Laurinat, Environmental Modeling Date

APPROVAL:

---

G. A. Morgan, Jr., Manager  
Chemical Flowsheet Development

Date

---

S. D. Fink, Director, Chemical Processing Sciences

Date

---

J. E. Occhipinti, Tank Farm Facility Engineering

Date

---

T. H. Huff, DWPF Engineering

Date

## EXECUTIVE SUMMARY

Two models were developed to predict maximum glycolate concentrations in the Savannah River Site (SRS) Concentration, Storage, and Transfer Facility (CSTF) from implementation of the Nitric-Glycolic flowsheet at the Defense Waste Processing Facility (DWPF). One model describes the kinetics of glycolate destruction via chemical oxidation with sodium permanganate. This model conservatively predicts glycolate concentration delivered to the CSTF with a high probability the actual glycolate concentration is lower than predicted. The second model describes the potential concentration of said residual glycolate within the 242-16H (i.e., “2H”) Evaporator system.

Previous testing has demonstrated the efficacy of a sodium permanganate strike to destroy glycolate in the DWPF Recycle Collection Tank (RCT) prior to transfer to Tank 22. Determination of the mechanistic chemical reaction confirmed the oxidant stoichiometry is effectively defined by the molar ratio of permanganate to glycolate (P/G). A kinetic model has been developed to conservatively predict P/G ratios and reaction durations required to reduce initial glycolate concentrations to a desired value in the RCT. This work indicates the following:

- Glycolate concentrations can be accurately predicted during the range of potential RCT strike and residence periods provided.
- The model can be used to predict glycolate concentration in the RCT in regions where testing is not feasible because it would lead to results below the analytical reporting limit.
- The model predicts that an assumed glycolate content of 35 to 65 mg/L with a P/G ratio = 20 can be reduced below 1.4 mg/L in 3 hours and below 0.24 mg/L at a 6 hour residence time.

Following the permanganate strike in the RCT, residual glycolate will enter the CSTF as a constituent in the recycle stream via Tank 22. It is assumed the highest concentrations of glycolate are achieved by recycle through the 2H evaporator system. A model is provided to conservatively estimate glycolate concentration factors across the 2H evaporator. Application of this model reveals:

- Molar concentration factors for both sodium and glycolate tend to decrease as a function of increasing initial sodium concentration.
- 95% of simulation results across all of the possible processing methodologies in the 2H system yield a glycolate concentration factor of 13.8 or less as a conservative estimate. Therefore, future processing is expected to lead to glycolate concentration factors of 13.8 or less

Consistent with and sequential to this effort is a 242-25H (i.e., “3H”) evaporator model (for glycolate concentration). This work is a discrete task, but a final document linking the expected glycolate destruction and concentration values across the 3H system will be provided. The calculations performed in this document should be re-evaluated in the event that DWPF RCT treatment procedures are modified.

## TABLE OF CONTENTS

LIST OF TABLES .....	viii
LIST OF FIGURES .....	viii
LIST OF ABBREVIATIONS.....	ix
1.0 Introduction.....	1
2.0 Experimental Data .....	2
2.1 Data Series.....	2
2.1.1 Glycolate Destruction via Chemical Oxidation in the RCT .....	2
2.1.2 Glycolate Destruction via Thermolysis in the CSTF .....	2
2.2 Quality Assurance .....	3
3.0 Results and Discussion .....	4
3.1 Kinetic Modeling of Glycolate Destruction .....	4
3.2 Application of Improved Glycolate Destruction Model.....	6
3.3 2H Evaporator Modeling.....	8
3.3.1 Development of the Continuous Flow Calculation for Concentration Factor Calculation.....	8
3.3.2 Definition of Inputs Required for Continuous-Flow Calculation.....	10
3.3.3 Estimation of Density as a Function of Salt Species Concentrations .....	12
3.3.4 Calculation Methodology .....	14
3.3.4.1 Initialization of Independent Variables.....	14
3.3.4.2 Calculation of Tank 22 Mass Fractions.....	16
3.3.4.3 Calculation of Tank 43 Molarities .....	17
3.3.4.4 Calculation of 2H Molarities.....	18
3.3.4.5 Calculation of Thermolytic Glycolate Degradation and Glycolate Concentration Factors .	19
3.3.5 Calculation Results.....	20
4.0 Conclusions and Recommendations .....	23
5.0 References.....	24
Appendix A : Glycolate analyses using OnGuard II H <sup>+</sup> and II Na <sup>+</sup> cartridges .....	A-1
Appendix B : Statistical Development of the Empirical Reaction Model .....	B-1

## LIST OF TABLES

Table 3-1. Predicted Glycolate Concentrations (mg/L) with Initial Glycolate Concentrations of 65 and 35 mg/L and P/G Ratios of 10, 20, 30, and 50. ....	8
Table 3-2. Independent Variable in the 2H Evaporator Model.....	11
Table 3-3. Component-Specific Constants for the Calculation of Apparent Specific Volume. ....	12

## LIST OF FIGURES

Figure 3-1: Comparison of Single and Two Term Models with SMECT Run.....	5
Figure 3-2: Effect of P/G Ratio on the Decline of Glycolate with Time. ....	7
Figure 3-3: Log Plots of Glycolate Concentration vs. Time with P/G Ratios of 20, 30 and 50. ....	8
Figure 3-4. Block Flow Diagram of Glycolate Pathway Through 2H Evaporator System.....	9
Figure 3-5. Necessary Parameters for Continuous Flow Calculation of Concentration Factors. ....	10
Figure 3-6. Plot of Calculated vs. Measured Densities from Historical Tank 22 (blue dot), Tank 38 (yellow dot), and Tank 43 (red dot) Samples. ....	13
Figure 3-7. Algorithm for Calculation of Glycolate Concentration Factors.....	14
Figure 3-8. Histograms of Nitrite, Nitrate, Hydroxide, and Carbonate Concentrations (M) in Tank 22 Since Dec. 31 <sup>st</sup> , 2009.....	15
Figure 3-9. Histograms of Nitrite, Nitrate, Hydroxide, and Carbonate Concentrations (M) Assumed in DWPF Recycle Material For 2H Evaporator Modeling.....	16
Figure 3-10. Mass Balance Around the 2H Evaporator System.....	17
Figure 3-11. Mass Balance Around 2H Evaporator Pot. ....	18
Figure 3-12. Sodium Concentration Factors Across the 2H Evaporator System Measured with 50,000 Simulations.....	21
Figure 3-13. Glycolate Concentration Factors Across the 2H Evaporator System Measured with 50,000 Simulations.....	22

## LIST OF ABBREVIATIONS

CSTF	Concentration, Storage, and Transfer Facilities
CSTR	Continuously-Stirred Tank Reactor
DWPF	Defense Waste Processing Facility
IC	Ion Chromatography
P/G	Permanganate to glycolate (initial molar ratio)
PSAL	Process Science Analytical Laboratory
RCT	Recycle Collection Tank
SME	Slurry Mix Evaporator
SMECT	Slurry Mix Evaporator Condensate Tank
SRAT	Sludge Receipt and Adjustment Tank
SRNL	Savannah River National Laboratory
SRR	Savannah River Remediation
SRS	Savannah River Site
SWPF	Salt Waste Processing Facility

## 1.0 Introduction

The Savannah River Site's Defense Waste Processing Facility (DWPF) is being upgraded with the introduction of the Nitric-Glycolic flowsheet. Glycolic acid has been shown to be superior to formic acid during chemical processing. The new flowsheet improves or maintains necessary parameters such as 1) reduction of mercury, 2) adjustment of feed rheology, 3) pH stability, and 4) adjustment of melter oxidation/reduction potential. Further, the potential for catalytic hydrogen generation in DWPF processing is virtually eliminated.<sup>1</sup>

DWPF process condensates are collected and returned to the SRS Concentration, Storage and Transfer Facilities (CSTF). The Recycle Collection Tank (RCT) collects off-gas condensate during chemical processing, vitrification, and other unit operations performed in DWPF and is the singular return vessel delivering recycle effluent back to CSTF. Each batch of recycle may contain a small amount of glycolate from chemical processing and melter off-gas condensates. To avoid potential flammability issues due to thermolysis of glycolate in the CSTF, Savannah River Remediation (SRR) tasked Savannah River National Laboratory (SRNL) to quantify and mitigate glycolate returns via DWPF's recycle stream.<sup>2</sup>

A Task Technical and Quality Assurance Plan was written to describe the testing requested by SRR in the development of a process to oxidize glycolate and other organic species that are responsible for hydrogen generation from thermolysis.<sup>3</sup> Laboratory scale studies using chemical simulants and radioactive waste samples have been completed as requested by a Technical Assistance Request<sup>4</sup> to evaluate the feasibility of using sodium permanganate to destroy glycolate in the RCT. The results from these laboratory studies were summarized in a series of reports.<sup>5-9</sup>

Tests at caustic conditions demonstrated sodium permanganate was effective in converting glycolate to oxalate, and permanganate ( $\text{Mn}^{7+}$ ) is reduced to manganate ( $\text{Mn}^{6+}$ ) with no significant formation of carbon dioxide or carbonate. Equation (1) was found to best describe the observed reaction of glycolate with permanganate under nominal and low glycolate entrainment conditions.<sup>7</sup>



Determination of the mechanistic chemical reaction confirmed the oxidant stoichiometry is effectively defined by the molar ratio of permanganate to glycolate (P/G). Testing confirmed that glycolate at starting concentrations ranging from 68 to 5100 mg/L, can be reduced below reportable limits of 10 to 100 mg/L respectively. This report describes the development and application of a kinetic model to conservatively predict P/G ratios and reaction durations required to reduce glycolate concentrations to a desired value in the RCT.

Following the permanganate strike in the RCT, residual glycolate will enter the CSTF as a constituent in the recycle stream via Tank 22. Given that glycolate has been observed to produce hydrogen gas in CSTF waste media,<sup>10</sup> it is important to understand the maximum concentration achievable in the CSTF. It is assumed the highest concentrations (excluding the 3H Evaporator systems) of glycolate is achieved by recycle through the 2H Evaporator system. This report provides a model to estimate glycolate concentration factors across the 2H Evaporator. A separate report will address glycolate concentration factors across the 3H Evaporator system.

## 2.0 Experimental Data

### 2.1 Data Series

#### 2.1.1 Glycolate Destruction via Chemical Oxidation in the RCT

Data used to model glycolate destruction using sodium permanganate in the RCT were sourced from previous studies on glycolate destruction using simulants<sup>7,8</sup> and radioactive waste samples.<sup>9</sup> All the tests had similar characteristics such as:

- Test batches were alkaline with most containing a small amount of Slurry Mix Evaporator (SME) product sludge or a SME simulant,
- Chemical processing at room temperature, typically around 20 °C,
- 20 minute addition time for the permanganate strike,
- Initial glycolate being in the range of 60 to 183 mg/L with 125 mg/L being common,
- P/G ratios ranging from 1.9 to 20,
- Sampling for at least 3 hours (with glycolate in later samples often below the analytical reporting limit of 10 mg/L),
- Samples being sulfite quenched when taken, and
- Essential data from each test included initial glycolate concentration, initial P/G ratio, and glycolate concentration as a function of time.

Glycolate values were removed from the database when observed at times after one or more results below the glycolate reporting limit. These values were considered an artifact of the analytical method due to the uncertainty in measurement near the reporting limit.

#### 2.1.2 Glycolate Destruction via Thermolysis in the CSTF

Recent testing performed at SRNL revealed the tendency of glycolate to thermolytically decompose in the presence of caustic waste media to form H<sub>2</sub> gas. This phenomenon was studied at a wide variety of conditions, allowing for the generation of an expression for hydrogen production via glycolate thermolysis, provided in Equation (2).<sup>11</sup>

$$\dot{v}_{H_2}^{glycolate} = 6.262 \times 10^5 [Na]^{1.520} [NO_3]^{0.282} [OH]^{1.441} [C_{gly}] e^{-82,300/RT} \quad (2)$$

where,

$\dot{v}_{H_2}^{glycolate}$  is the hydrogen generation rate in ft<sup>3</sup> h<sup>-1</sup> gal<sup>-1</sup> (standard conditions: 25 °C, 1 atm),

$[Na]$  is the supernatant concentration of sodium in mol L<sup>-1</sup>,

$[NO_3]$  is the supernatant concentration of nitrate in mol L<sup>-1</sup>,

$[OH]$  is the supernatant concentration of hydroxide in mol L<sup>-1</sup>,

$[C_{gly}]$  is the supernatant concentration of carbon from glycolate in mol L<sup>-1</sup>,

$R$  is the ideal gas constant, 8.314 J mol<sup>-1</sup> K<sup>-1</sup>, and

$T$  is the temperature in K.

Given that the hydrogen observed from thermolysis is from the degradation of glycolate, the rate of glycolate destruction by thermolysis is necessarily greater than or equal to the rate of hydrogen formation. Therefore, the expression given in Equation (2) may be used to conservatively predict the degradation rate

of glycolate in caustic waste with the assumption that one mole of glycolate is destroyed for every mole of hydrogen liberated. The equation for thermolytic glycolate destruction rate in mol L<sup>-1</sup> min<sup>-1</sup> is given in Equation (3).

$$\frac{d[Gly]}{dt} = -6.38 \times 10^{-3} [Na]^{1.520} [NO_3]^{0.282} [OH]^{1.441} [Gly] e^{-82,300/RT} \quad (3)$$

where,

$[Gly]$  is the supernatant concentration of glycolate in mol L<sup>-1</sup>, and

$\frac{d[Gly]}{dt}$  is the time-derivative of glycolate concentration in mol L<sup>-1</sup> min<sup>-1</sup>.

Equation (3) is used in the remainder of this report to approximate the degradation of glycolate in caustic waste following transfer to Tank 22 from the RCT. This information is used to ascertain the maximum glycolate concentration factor (as defined in Equation (4)) achievable in the 2H Evaporator system.

$$f_{gly} = \frac{[Gly]_{2H}^{Output}}{[Gly]_{22}^{Input}} \quad (4)$$

where,

$f_{gly}$  is the glycolate concentration factor,

$[Gly]_{2H}^{Output}$  is the glycolate concentration exiting the 2H Evaporator system in mol L<sup>-1</sup>, and

$[Gly]_{22}^{Input}$  is the glycolate concentration entering Tank 22 from the RCT in mol L<sup>-1</sup>.

## 2.2 Quality Assurance

The TTR for this work specified the testing has a functional class of Safety Class.<sup>2</sup> Requirements for performing reviews of technical reports and the extent of review are established in manual E7 2.60. SRNL documents the extent and type of review using the SRNL Technical Report Design Checklist contained in WSRC-IM-2002-00011, Rev. 2.

Commercial software JMP Pro Version 11.2.1<sup>12</sup> and Mathematica Version 12.0.0<sup>13</sup> were used in the kinetic modelling as described below. JMP software is classified as Level D.<sup>14</sup> The outputs included from both software packages were independently verified using an alternate software package as part of the design verification meeting the requirements for safety significant work.

Modeling of the 2H Evaporator concentration factors was accomplished by performing several thousand calculations of the concentration factor at randomly-generated initial conditions. These calculations were performed en masse by using the Octave 5.2.0 Integrated Development Environment. Octave 5.2.0 has not been evaluated for a software classification for use at SRS, so a subset of calculations was technically reviewed via design verification by alternate calculations (per technical review requirements in E7, 2.60) to ensure accuracy.

### 3.0 Results and Discussion

#### 3.1 Kinetic Modeling of Glycolate Destruction

The goal of modeling the experimental data for glycolate oxidation was to predict residual glycolate as a function of initial glycolate and P/G ratio to provide a conservative estimate of glycolate removal. Residual glycolate will increase thermolytic hydrogen production in the SRS Tank Farm. Tank Farm modeling needs a bound on expected residual glycolate from implementation of the Nitric-Glycolic flowsheet at DWPF.

Zamecnik et al.<sup>7</sup> examined kinetic models for the permanganate oxidation of glycolate. One model applied to their data set was first order in each of glycolate and permanganate. This approach is reasonable since both species are relatively dilute in the RCT batch to be processed. The species would react when one molecule of permanganate finds a molecule of glycolate in solution. The basic model expression was:

$$d[G]/dt = -K * [G] * [P] \quad (5)$$

where,

[G] is glycolate concentration in mmol L<sup>-1</sup>,  
 [P] is permanganate concentration in mmol L<sup>-1</sup>,  
 t is time in minutes, and  
 K is a kinetic rate constant in L mmol<sup>-1</sup> min<sup>-1</sup>.

Concentrations would be in mmol/L though the reference used mmol/kg. This model has an analytical solution where G(t) can be obtained explicitly and where that solution can be inverted to obtain t as an explicit function of G. Zamecnik et al.<sup>7</sup> found that their “Reagent” and dilute Sludge Receipt and Adjustment Tank (SRAT) product tests supported a stoichiometric ratio of P/G of 4 to 1. Use of permanganate for the oxidation appeared more efficient if sludge was present in the feed batch. The Zamecnik report discusses the possibility that manganese in the sludge interacts with permanganate to produce Mn<sup>+3</sup>, an efficient oxidizer that might enhance the kinetics of glycolate destruction.

Contrary to initial results from experiments with simulants, experiments using radioactive waste samples found formate reacting with permanganate in the process.<sup>9</sup> A review of the analytical methods used to detect organic species for the simulant studies was conducted (see Appendix A). A reevaluation of the data using the revised methods noted formate reacting with permanganate in the simulant studies.

To account for the presence of reactions with other species, the current work explored a model with an additional loss term for permanganate. The model with a loss term involving a rate term K<sub>x</sub> provides two equations shown below. Equation (6) has the “4” in its first term to account for stoichiometry of permanganate to glycolate as discussed in Zamecnik et al.<sup>7</sup> Oxidizing one mole of glycolate consumes four moles of permanganate ion in that stoichiometry.

$$d[P]/dt = -K_1 * 4 * [G] * [P] - K_x * [P] \quad (6)$$

$$d[G]/dt = -K_1 * [G] * [P] \quad (7)$$

The equations together do not have an analytical equation involving time, but they can be partially solved analytically if Equation (6) is divided by Equation (7). The calculational method is demonstrated by Benson in his work on kinetics modeling<sup>15</sup>. The resulting equation for d[P]/d[G] can be integrated to obtain:

$$[P - P_0] = 4 * [G - G_0] + (K_x / K_1) * \ln(G / G_0) \quad (8)$$

Here the zero subscripts denote permanganate and glycolate at time zero. Equations (6) and (7) can be combined to produce a term that must be integrated numerically to obtain results in time. It is an initial value problem requiring P<sub>0</sub>, G<sub>0</sub>, and the two rate constants. Experiments often would report G<sub>0</sub> and an initial

P/G ratio.  $P_0$  would thus be the product of P/G ratio times  $G_0$ . The equation to be integrated is shown in Equation (9).

$$d[G]/dt = -K_1 * [G] * [(P_0 + 4 * (G - G_0) + (K_x / K_1) * \ln(G / G_0))] \quad (9)$$

G is the variable of integration and time only appears in the differential. Dividing both sides of Equation (9) by the right hand side and multiplying by dt separates the variables, but the resulting left side has no analytical integral such as would be found in a table of integrals.

The model with permanganate loss term, equations 6 and 7, was found to fit data better than the second order model expressed in Equation (5) without permanganate loss. This model with loss term is referred to as the “current model” in this report. Figure 3-1 shows results using both models to extrapolate glycolate decay curves using data from prior testing with Slurry Mix Evaporator Condensate Tank (SMECT) waste from DWPF. Equation (5), a second order kinetic equation with no permanganate loss term, overpredicts the experimental data early in the reaction and underpredicts it later. The theoretical model with loss term (i.e. current model, equations 6 and 7) captures the shape of the data best. The important issue for the model with loss term is that it does better at fitting experimental data late in the process where ability to predict residual glycolate is most important. The goal is to have a model that is mechanistic late in the reaction so that it does not underestimate residual glycolate. Equations (6) and (7) together provide a second order mechanism including a permanganate loss term.

The radioactive SMECT test data was used to fit the current model because that data set was found to have slow glycolate destruction kinetics relative to the body of nonradioactive data and also the radioactive OGCT test. The current model bounds 84% of the body of data with 95% confidence as explained below and in Appendix B. Exhibit 4 of Appendix B provides the statistics for the confidence result.

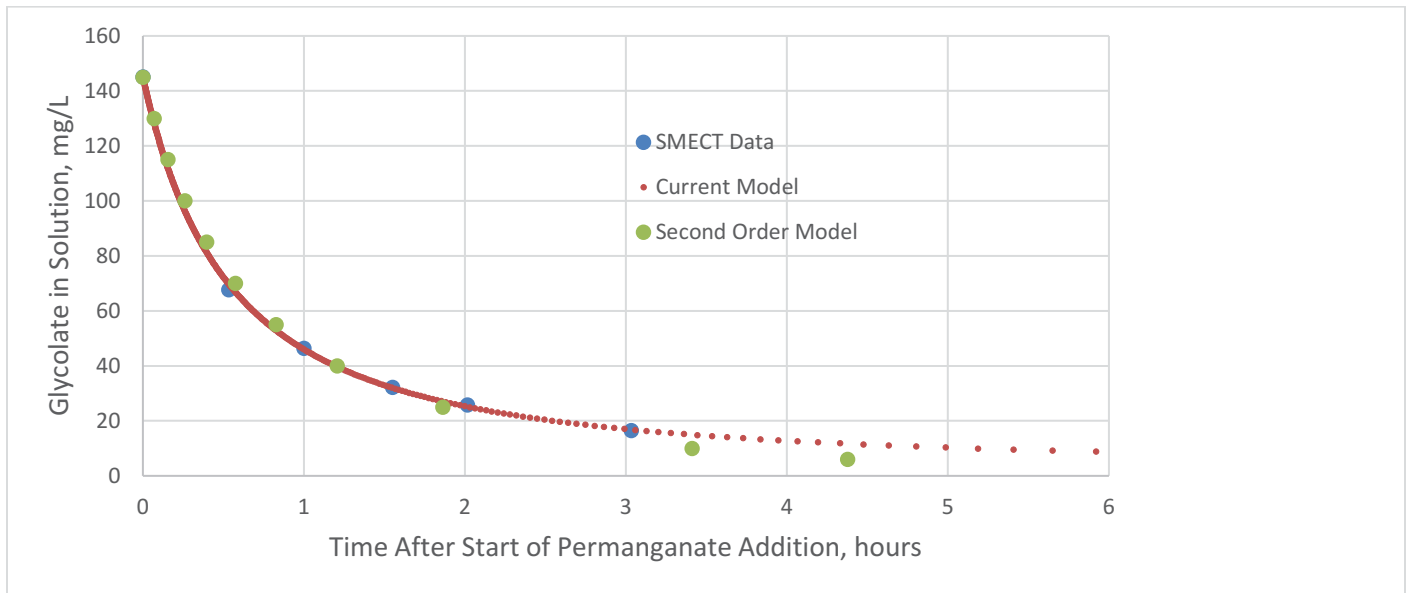


**Figure 3-1: Comparison of Single and Two Term Models with SMECT Run**

A key goal of modeling the glycolate oxidation kinetics is to produce a mechanistic model that predicts glycolate concentration on the high side of what is realized with time. This is referred to as “conservative” in this report because it is desired to reduce glycolate concentration below measurable values to reduce thermolytic hydrogen downstream. The second order model from the Zamecnik report<sup>7</sup> and the current

model are both mechanistic, being based on chemical rate laws. The approach for conservative estimation of residual glycolate used the following steps:

1. Use JMP® software<sup>12</sup> and a regression fit that could be handled by JMP® to evaluate uncertainties of modeling.
2. Fit the current model of Equations (6) and (7) with the SMECT real waste data only to obtain a  $K_1$  and  $K_x$ .<sup>13</sup> The SMECT run was found to be conservative (slow glycolate destruction kinetics) when compared with the body of simulant and real waste data. The body of simulant and radioactive waste sample data is thereby represented by a regression fit that is only used for JMP application.
3. The regression fit can only be used within the range of data used to fit it. The fit is only used with JMP® to evaluate the level of conservatism of the current model.
4. The SMECT model with loss term is shown to be conservative with respect to the body of data and regression fit that was used.
5. The current model fit to the SMECT data set is then used to make conservative predictions of residual glycolate in liquid product to be sent to the Tank Farm.

Additional information on data processing and statistical development are in Appendix B. The theoretical model is shown to be a conservative predictor of G compared to the body of 95 data points (26 simulant tests and 2 real waste tests). Several of the tests only have measured data early on because glycolate dropped below the reporting limit of 10 mg/L. Note also that there are two experiments called 7a because that designator was used for different data sets in the simulant tests.

### 3.2 Application of Improved Glycolate Destruction Model

The SMECT data are successfully fit with a model with rate constants  $K_1 = 0.00286 \text{ min}^{-1} \text{ mM}^{-1}$  and  $K_x = 0.00276 \text{ min}^{-1}$  (see Appendix B, Exhibit 3). Figure 3-2 plots the SMECT model predictions of glycolate concentrations as a function of reaction time for an initial glycolate concentration of 60 mg/L and varying P/G ratios. The model predicts that as initial P/G ratio moves from 6 to 9, glycolate rapidly descends from 60 mg/L to less than 5 mg/L in 4 – 6 hours. Using a higher P/G ratio reduces glycolate concentrations even faster as expected.

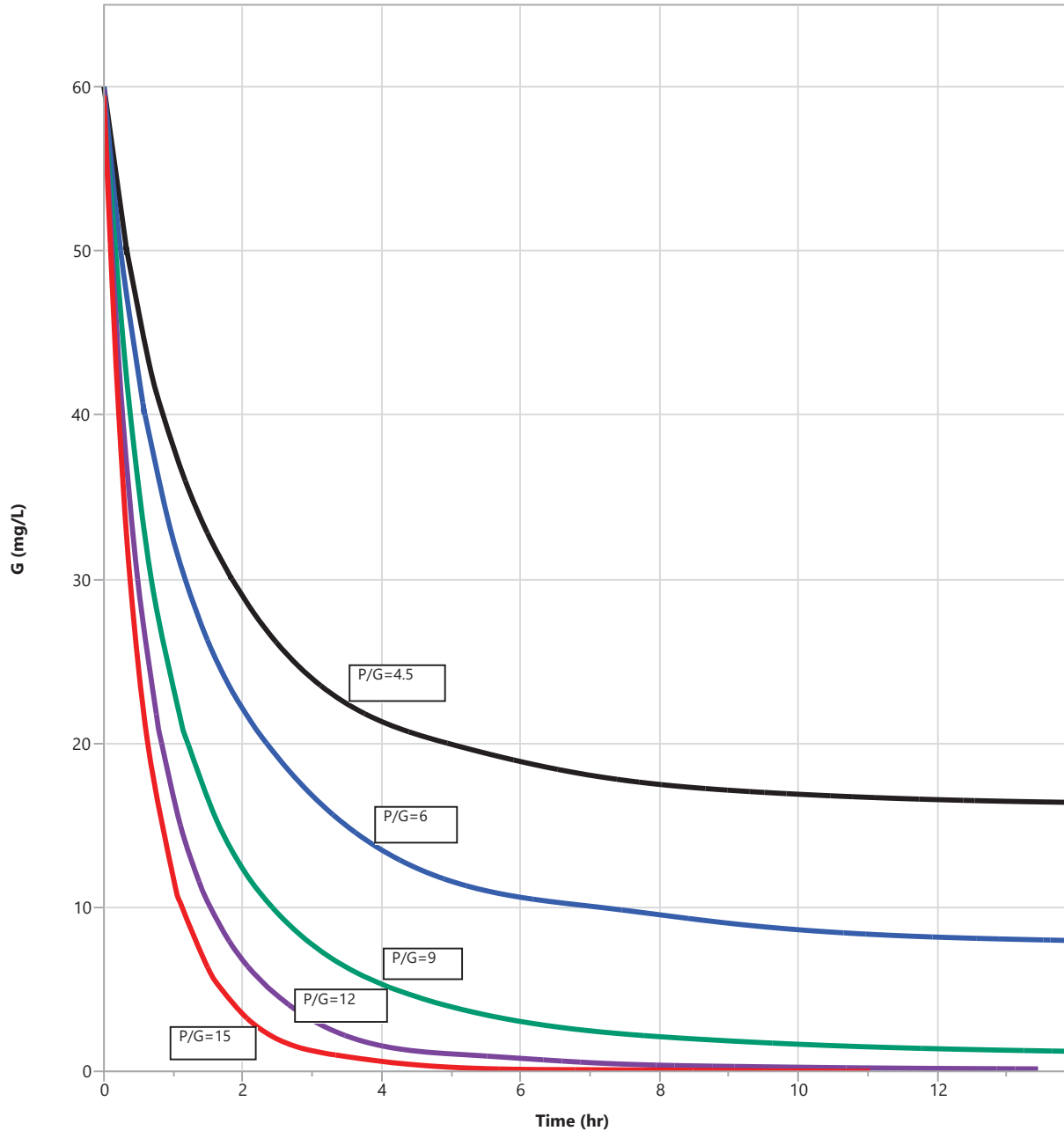


**Figure 3-2: Effect of P/G Ratio on the Decline of Glycolate with Time.**

The theoretical model was used to predict glycolate concentrations below what can currently be measured in a laboratory. Cases considered assumed initial glycolate concentrations of 65 mg/L (0.87 mM) and 35 mg/L (0.47 mM). Table 3-1 shows these results for high P/G ratios as labeled. Figure 3-3 shows base 10 log plots that allow estimation of the very low glycolate concentrations that result from these batch reactions.

**Table 3-1. Predicted Glycolate Concentrations (mg/L) with Initial Glycolate Concentrations of 65 and 35 mg/L and P/G Ratios of 10, 20, 30, and 50.**

Initial Glycolate = 35 mg/L						
P/G Ratio	T = 0	2 Hours	3 Hours	4 Hours	6 Hours	8 Hours
10	3.50E+01	1.15E+01	8.06E+00	6.10E+00	4.08E+00	3.12E+00
20	3.50E+01	3.30E+00	1.43E+00	7.08E-01	2.39E-01	1.10E-01
30	3.50E+01	8.97E-01	2.30E-01	7.25E-02	1.19E-02	3.27E-03
50	3.50E+01	6.18E-02	5.48E-03	6.97E-04	2.77E-05	2.76E-06
Initial Glycolate = 65 mg/L						
P/G Ratio	T = 0	2 Hours	3 Hours	4 Hours	6 Hours	8 Hours
10	6.50E+01	9.66E+00	5.36E+00	3.33E+00	1.63E+00	9.45E-01
20	6.50E+01	9.34E-01	2.00E-01	5.33E-02	6.93E-03	1.59E-03
30	6.50E+01	7.94E-02	6.30E-03	7.34E-04	2.51E-05	2.24E-06
50	6.50E+01	5.34E-04	5.85E-06	1.26E-07	3.16E-10	4.27E-12

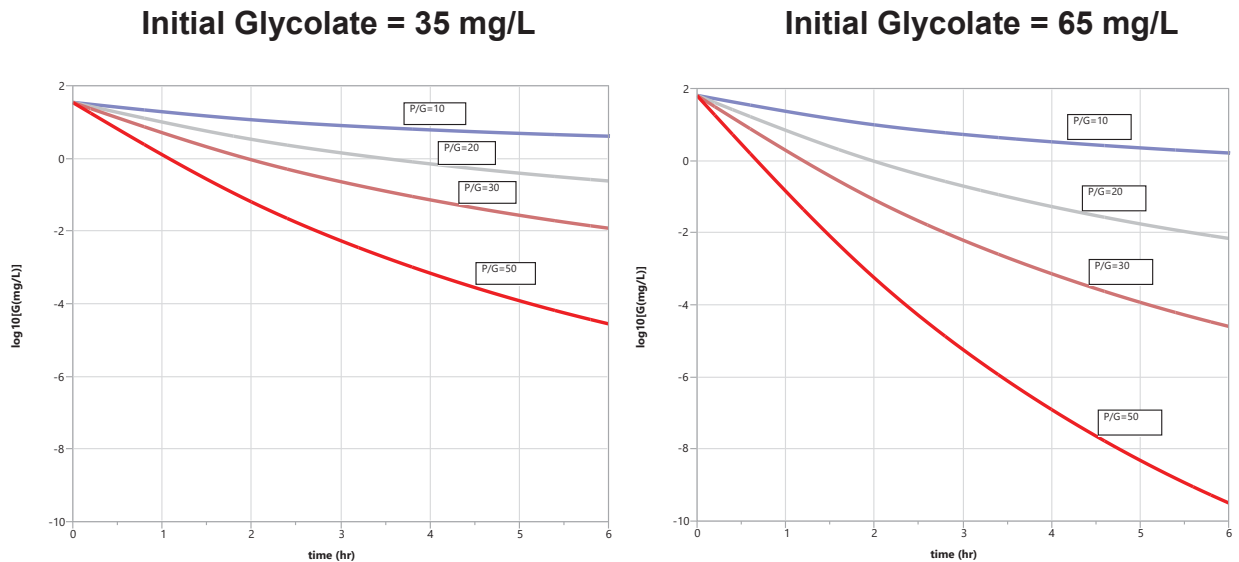


**Figure 3-3: Log Plots of Glycolate Concentration vs. Time with P/G Ratios of 20, 30 and 50.**

### 3.3 2H Evaporator Modeling

#### 3.3.1 *Development of the Continuous Flow Calculation for Concentration Factor Calculation*

Following the permanganate strike in the RCT, glycolate is expected to enter the CSTF as a constituent in the recycle stream via Tank 22. Given that glycolate has been observed to produce hydrogen gas in CSTF waste media and that the production of hydrogen has been shown to be linearly dependent on glycolate concentration, it is important to understand the maximum concentration achievable in the CSTF.<sup>11</sup> The work presented here (determination of glycolate concentration factors across the 2H Evaporator) is the first step in this process.

It has been shown that Tank 22, the initial receipt tank for DWPF recycle material, is sufficiently dilute to mitigate any concerns of flammability due to glycolate thermolysis.<sup>10</sup> Transfers of glycolate-containing Tank 22 material to most tanks would result in further dilution of glycolate leading to a concentration factor (as defined in Equation (4)) of less than 1; these scenarios are therefore not applicable for consideration of the maximum concentration factor. Transfers of DWPF recycle material from Tank 22 to the 3H Evaporator system (which is capable of higher temperatures and higher concentrations) are currently protected by the Evaporator Feed Qualification program. For this reason, transfers to the 3H system are considered less likely than transfers to the 2H system, and are therefore not considered here (concentration factors across the 3H system will be evaluated in a separate document). The most likely point of concentration for glycolate in the CSTF is the 2H Evaporator system, which is currently dedicated to the concentration of DWPF recycle material. A block flow diagram of tanks involved in this transfer is given in Figure 3-4.

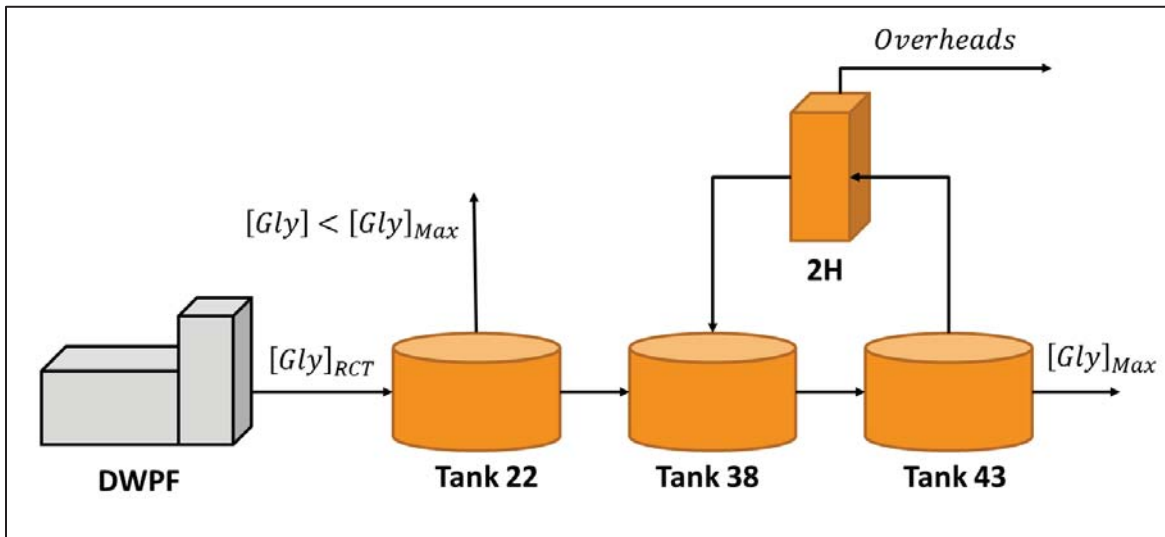


**Figure 3-4. Block Flow Diagram of Glycolate Pathway Through 2H Evaporator System.**

The block flow diagram in Figure 3-4 portrays the expected flow of glycolate-containing recycle material from DWPF through Tank 22 and into the 2H Evaporator system. The expected operation order is as follows:

1. Glycolate-containing waste is transferred from the DWPF RCT to Tank 22.
2. From Tank 22, the glycolate-containing waste may be transferred to the 2H system via Tank 38 (for concentration) or to other waste tanks in the CSTF (for dilution).
3. Tank 38 material is transferred to Tank 43 (the 2H feed tank).
4. Tank 43 material is transferred to the 2H Evaporator for concentration.
5. The concentrated waste in the 2H Evaporator is transferred to Tank 38 (the 2H drop tank).
6. Concentrated waste in Tank 38 is recycled to Tank 43 for further concentration.
7. Occasional transfers are made from Tank 43 to other waste tanks to de-inventory the 2H system.

The block flow diagram shown in Figure 3-4 is the basis for the calculations performed to determine a maximum glycolate concentration factor. For the purposes of this report, the system described is approximated as a continuous-flow operation. This assumption is believed to be a conservative approximation of the time-averaged behavior of the 2H system over the timeframe required (~months to years) to build-up glycolate concentrations to appreciable levels in these multiple tanks. Note that the selection of Tank 38 as a 2H entry point and Tank 43 as a 2H exit point, while realistic with respect to

previous years of operation, is not strictly required; Tank 22 material may be fed to Tank 43 and 2H material inventory may be decanted from Tank 38 with minimal impact to the predictions made with this model.

### 3.3.2 Definition of Inputs Required for Continuous-Flow Calculation

The block flow diagram in Figure 3-4 is replicated in Figure 3-5 with additional parameters necessary for the continuous-flow calculation identified.

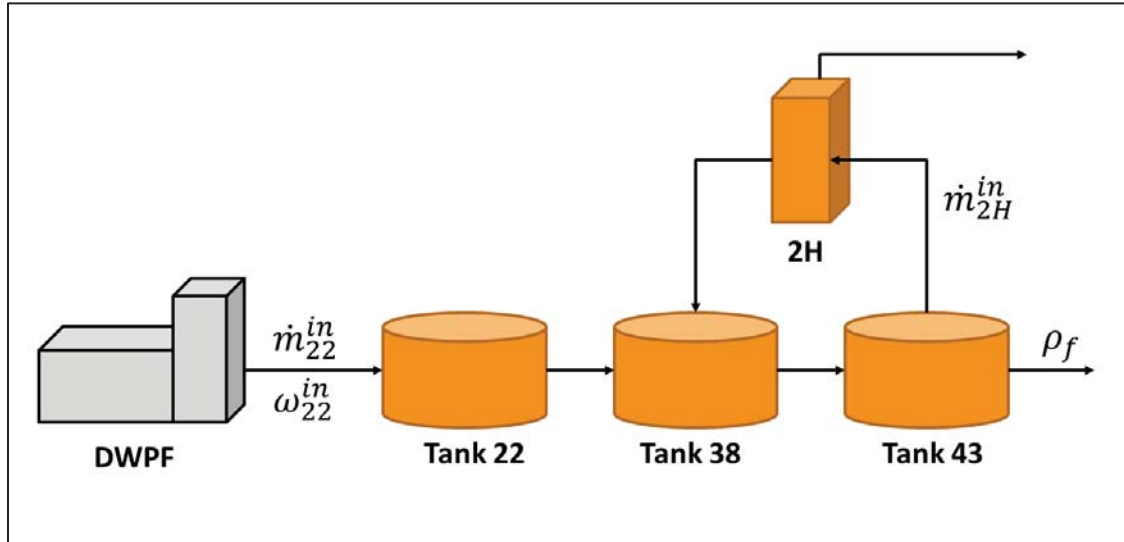


**Figure 3-5. Necessary Parameters for Continuous Flow Calculation of Concentration Factors.**

The parameters identified in Figure 3-5 are the only independent variables present in the system. These variables are defined in Table 3-2 along with assumed values for each independent parameter.

**Table 3-2. Independent Variable in the 2H Evaporator Model.**

Parameter	Description	Value	Sensitivity <sup>†</sup>
$\dot{v}_{22}^{in}$	Flow rate of recycle material into Tank 22	1.4 – 2.3 gal min <sup>-1</sup>	+
$[Gly]_{RCT}$	Concentration of Glycolate from the RCT	5 mg L <sup>-1</sup>	N/A
$\omega_{22}^{in}$	Composition of material in DWPF recycle stream	0.1507 ≤ [NO <sub>2</sub> ] ≤ 0.5528 mol L <sup>-1</sup> 0.0475 ≤ [NO <sub>3</sub> ] ≤ 0.5924 mol L <sup>-1</sup> 0.1519 ≤ [OH] ≤ 1.0065 mol L <sup>-1</sup> 0.0188 ≤ [CO <sub>3</sub> ] ≤ 0.1040 mol L <sup>-1</sup>	-
$V_{22}$	Volume of Tank 22	250,000 – 950,000 gal	-
$T_{22}$	Temperature of Tank 22	23 – 27 °C	-
$V_{38}$	Volume of Tank 38	210,000 – 960,000 gal	-
$T_{38}$	Temperature of Tank 38	25 – 37 °C	-
$V_{43}$	Volume of Tank 43	520,000 – 1,050,000 gal	-
$T_{43}$	Temperature of Tank 43	25 – 35 °C	-
$\dot{v}_{2H}^{in}$	Flow rate of material fed to 2H Evaporator	10 – 25 gal min <sup>-1</sup>	+
$V_{2H}$	Volume of 2H Evaporator	1,738 gal	-
$T_{2H}$	Temperature of 2H Evaporator	110 °C	-
$\rho_f$	Density of material leaving Tank 43	1.122 – 1.421 g mL <sup>-1</sup>	+

<sup>†</sup>Sensitivity is defined here as the sign of the derivative of the glycolate concentration factor with respect to the variable in question. A sign of “+” indicates that when the variable is increased, the glycolate concentration factor would be expected to increase. A sign of “-” indicates that when the variable is increased, the glycolate concentration factor would be expected to decrease.

The ranges for variables  $V_{22}$ ,  $T_{22}$ ,  $V_{38}$ ,  $T_{38}$ ,  $V_{43}$ ,  $T_{43}$ ,  $V_{2H}$ , and  $T_{2H}$  were chosen based on recommendations from SRR. The input for these variables into the glycolate molar concentration factor are randomly generated from a rectangular distribution (equal probability for all values) within the ranges specified. The range for variable  $\dot{v}_{22}^{in}$  was chosen based on time-averaged estimates of anticipated annual recycle volumes under the Salt Waste Processing Facility (SWPF) flowsheet. The value of 1.4 gal min<sup>-1</sup> corresponds to a minimum anticipated annual volume of 750,000 gal yr<sup>-1</sup>, while the value of 2.3 gal min<sup>-1</sup> corresponds to a maximum anticipated annual volume of 1,200,000 gal yr<sup>-1</sup>. The range for variable  $\dot{v}_{2H}^{in}$  was chosen based on discussion with SRR wherein the range of 15 – 25 gal min<sup>-1</sup> was identified as the volume feed rate to the 2H Evaporator. A lower bound of 10 gal min<sup>-1</sup> is used to approximate an outage time of 4 months. The value of  $[Gly]_{RCT}$  was chosen based on the discussion of permanganate kinetics presented earlier in this report. Values for  $\omega_{22}^{in}$  and  $\rho_f$  were chosen from sample records reported in the NTANK database.<sup>16</sup> Measured values of nitrite, nitrate, hydroxide, and carbonate from Tank 22 samples as well as density measurements from Tank 43 and Tank 38 supernatant material from samples taken since January 1<sup>st</sup>, 2010 were compiled and used to generate a distribution representative of observed waste tank chemistry. These distributions were used to randomly generate values for each of the specified independent

variables for each calculation of the glycolate molar concentration factor. Note that while 110 °C was recommended for use by SRR personnel as a temperature for the 2H Evaporator system, average temperatures required to achieve the densities examined in this report are expected to exceed this value.

### 3.3.3 Estimation of Density as a Function of Salt Species Concentrations

In the process of performing the calculation of a glycolate concentration factor across the 2H Evaporator system, it is necessary to estimate the density as a function of changing salt concentrations. Specifically, it is necessary to estimate the density of Tank 22 and Tank 43 material. This was accomplished using a temperature-dependent electrolyte solution density model put forward by Laliberte and Cooper.<sup>17</sup> In this model, the density of an electrolyte solution may be approximated according to Equation (10):

$$\rho_{solution} = \frac{1}{\frac{\omega_{H_2O}}{\rho_{H_2O}} + \sum_i \omega_i \bar{v}_{app,i}} \quad (10)$$

where,

$\rho_{solution}$  is the density of the electrolyte solution in kg m<sup>-3</sup>,

$\rho_{H_2O}$  is the density of water in kg m<sup>3</sup>,

$\omega_{H_2O}$  is the mass fraction of water in the electrolyte solution,

$\omega_i$  is the mass fraction of salt component “i” in the electrolyte solution, and

$\bar{v}_{app,i}$  is the apparent specific volume of salt component “i” in the electrolyte solution in m<sup>3</sup> kg<sup>-1</sup>.

In the Laliberte-Cooper Density Model, the apparent specific volume,  $\bar{v}_{app,i}$ , is calculated as a function of temperature according to Equation (11):

$$\bar{v}_{app,i} = \frac{\omega_i + c_{2,i} + c_{3,i}T}{(c_{0,i}\omega_i + c_{1,i})e^{(0.000001(T+c_{4,i})^2)}} \quad (11)$$

where,

$T$  is the temperature in °C, and  $c_{0,i}$  -  $c_{4,i}$  are component-specific empirical constants.

For the purposes of the evaluations described in this report, only those components present at appreciable concentrations are considered in the calculation of density (i.e., sodium nitrate, sodium nitrite, sodium hydroxide, and sodium carbonate). The component-specific empirical constants for each of these salt species is given in Table 3-3.<sup>17</sup>

**Table 3-3. Component-Specific Constants for the Calculation of Apparent Specific Volume.**

Compound, i	$c_{0,i}$	$c_{1,i}$	$c_{2,i}$	$c_{3,i}$	$c_{4,i}$
NaNO <sub>2</sub>	78.365	298.00	0.96246	0.0021999	1500.00
NaNO <sub>3</sub>	49.209	94.737	0.77927	0.0075451	1819.2
NaOH	385.55	753.47	-0.10938	0.0006953	542.88
Na <sub>2</sub> CO <sub>3</sub>	0.012755	0.014217	-0.091456	0.0021342	3342.4

The Laliberte-Cooper density model was compared to previous density measurements made at SRS to determine the validity of using this model to approximate SRS waste. Historic records from Tank 22, Tank 38, and Tank 43 samples where density and concentrations of nitrite, nitrate, and hydroxide were reported were compiled and evaluated against the Laliberte-Cooper density model. The results of this comparison are displayed graphically in Figure 3-6.

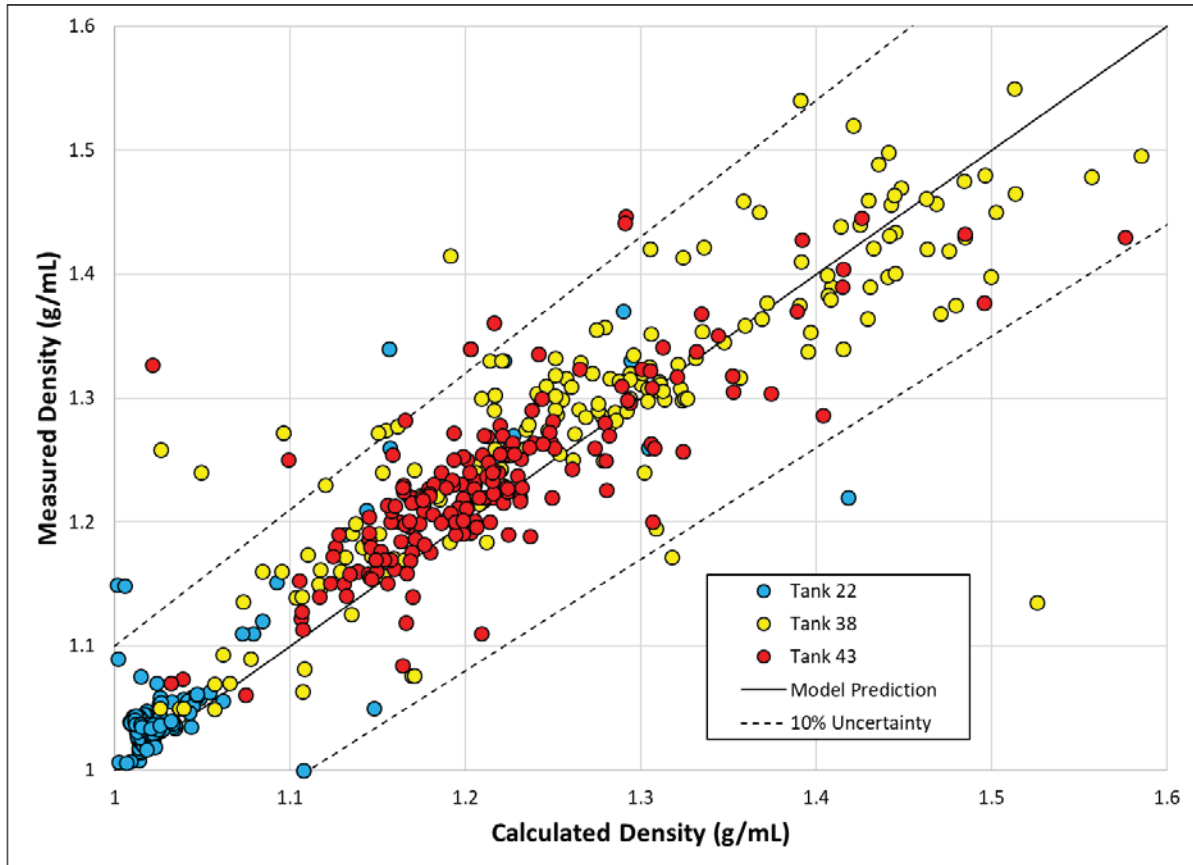


**Figure 3-6. Plot of Calculated vs. Measured Densities from Historical Tank 22 (blue dot), Tank 38 (yellow dot), and Tank 43 (red dot) Samples.**

As shown in Figure 3-6, the Laliberte-Cooper density model neatly bisects the historical measurements of density made from Tank 22, Tank 38, and Tank 43 sample material. The majority of the Tank 22, 38, and 43 measurements fall within 10% of the model prediction, suggesting that the model is capable of predicting density within the error associated with a density measurement (10%). This is a confirmation of the model's adequacy to describe density of SRS waste material as a function of salt composition. Note that more points appear to fall above the 10% uncertainty region than fall below it, suggesting that the model has a tendency to underpredict density. This underprediction is likely due to the fact that only nitrite, nitrate, and hydroxide were considered for the model comparison (other salt components were likely present and not considered in the analysis) and is conservative for the calculation of glycolate concentration factors relative to the calculation of concentration factors using real densities. It should also be noted that some of the points below the 10% uncertainty region are likely results of erroneous density measurements (e.g., one Tank 38 sample recorded a density of 1.1355 g/mL and concentrations of 1.7 M NaNO<sub>2</sub>, 1.53 M NaNO<sub>3</sub>, and 6.69 M NaOH, which is predicted to have a density of greater than 1.3 by OLI).

### 3.3.4 Calculation Methodology

The calculation of glycolate concentration factors proceeds according to the algorithm presented in Figure 3-7.

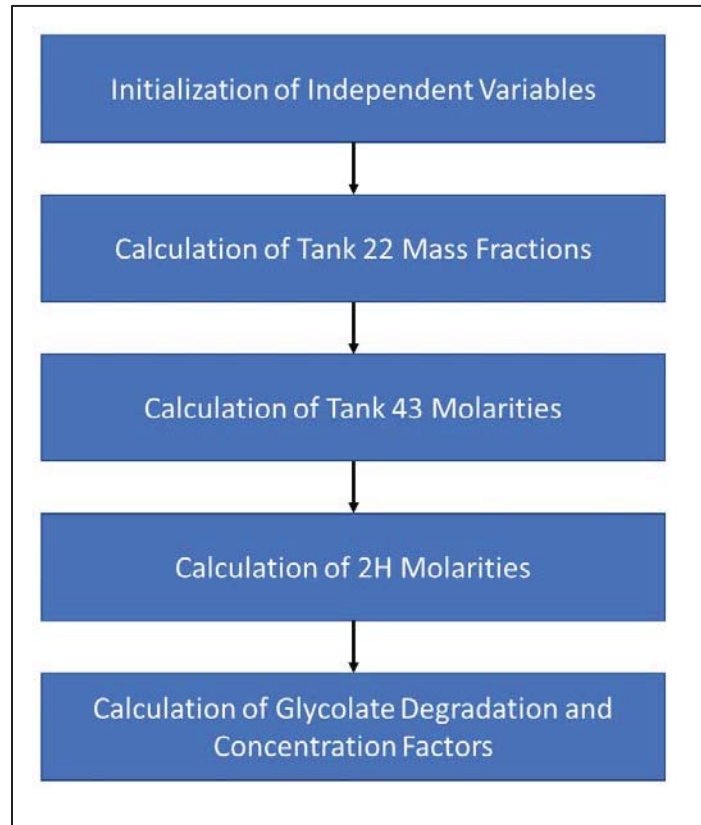


**Figure 3-7. Algorithm for Calculation of Glycolate Concentration Factors.**

The steps identified in Figure 3-7 are explained in further detail in the sections that follow.

#### 3.3.4.1 Initialization of Independent Variables

The independent variables identified in Table 3-2 must first be initialized before a calculation of glycolate concentration factor can be performed. Variables  $\dot{v}_{22}^{in}$ ,  $V_{22}$ ,  $T_{22}$ ,  $V_{38}$ ,  $T_{38}$ ,  $V_{43}$ ,  $T_{43}$ ,  $\dot{v}_{2H}^{in}$ , and  $\rho_f$  are generated from square distributions of the ranges provided in Table 3-2. Variables  $V_{2H}$  and  $T_{2H}$  are provided as constants with values specified in Table 3-2.

The variable salt concentrations in the DWPF recycle stream (specified as  $\omega_{22}^{in}$  in Table 3-2) are generated from a random distribution that is equivalent to the distribution of nitrate, nitrate, hydroxide, and carbonate measurements made of every Tank 22 sample since 2009. Histograms of Tank 22 sample measurements of nitrite, nitrate, hydroxide, and carbonate molarity since 2009 are given in Figure 3-8.

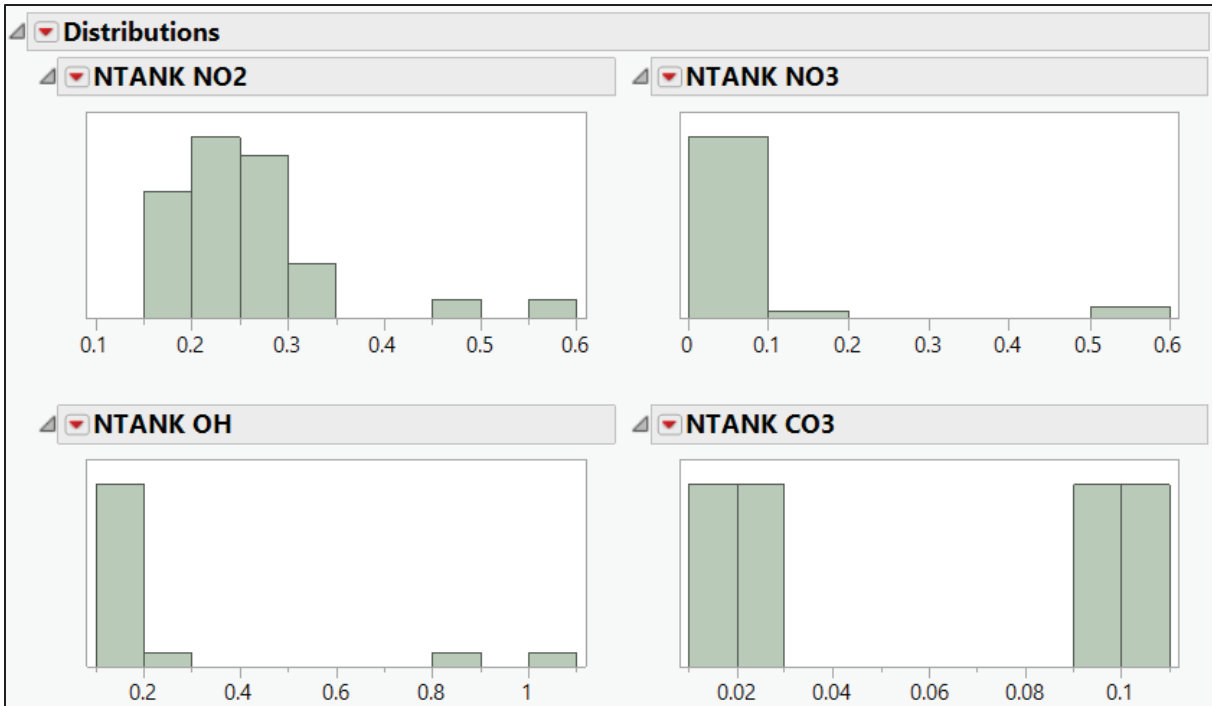


**Figure 3-8. Histograms of Nitrite, Nitrate, Hydroxide, and Carbonate Concentrations (M) in Tank 22 Since Dec. 31<sup>st</sup>, 2009.**

Note in Figure 3-8 that nitrite, nitrate, and hydroxide distributions are relatively well-behaved. Tank 22 nitrite concentrations measured since 2009 have primarily varied between 0.15 and 0.35 M, with occasional excursions above 0.45 M (recall that the floor of 0.15 M is artificial in the case of nitrite and hydroxide). Nitrate and hydroxide molarities are also primarily limited to a single concentration region (<0.2 M) with occasional excursions to greater than 0.5 M (in the case of nitrate) and 0.8 M (in the case of hydroxide). The distribution of carbonate is poorly defined and appears to be a square distribution with binodal behavior (50% of measurements occurring below 0.03 M and 50% of measurements occurring above 0.09 M). This observation is due to the limited available data of carbonate concentrations going back to 2009 (only four measurements have been reported).

Histograms of concentrations for each species used in 2H modeling calculations are given in Figure 3-9 for comparison.

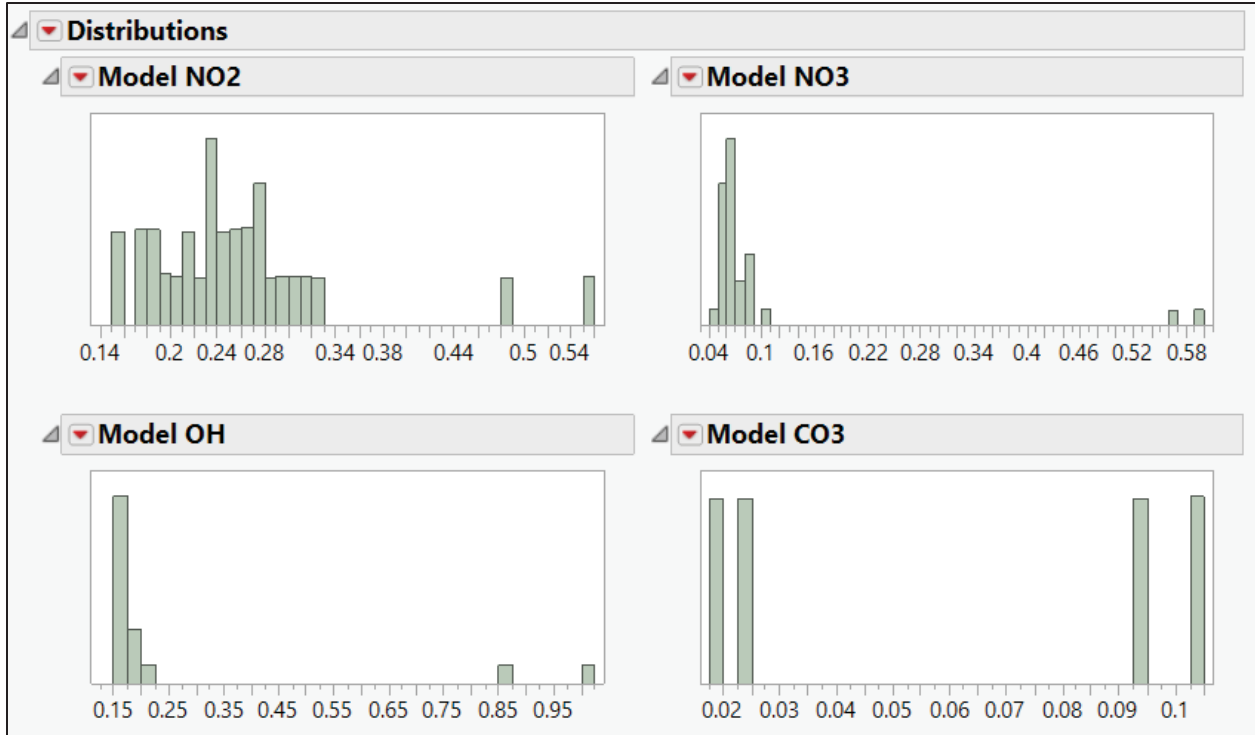


**Figure 3-9. Histograms of Nitrite, Nitrate, Hydroxide, and Carbonate Concentrations (M) Assumed in DWPF Recycle Material For 2H Evaporator Modeling.**

The histograms shown in Figure 3-9 agree well with those shown in Figure 3-8, indicating that the distributions of nitrite, nitrate, hydroxide, and carbonate concentrations (M) assumed in DWPF recycle material during 2H Evaporator system modeling are sufficiently realistic compared to the frequencies of corresponding measurements in Tank 22 supernate since 2009.

### 3.3.4.2 Calculation of Tank 22 Mass Fractions

An approximation of Tank 22 density is required to calculate the mass fractions of each salt component in Tank 22. Given that the calculation of density according to the Laliberte-Cooper model requires knowledge of the salt component mass fractions, a non-linear equation can be established and solved for the calculation of density and subsequent mass fractions. The non-linear equation is established below in Equation (12).

$$f(\rho_{solution}) = 0 = \rho_{solution} - \frac{0.001}{\left( \frac{1 - \sum_i \frac{[i]MW_i}{1000\rho_{solution}}}{\rho_{H_2O}} + \sum_i \frac{[i]MW_i}{1000\rho_{solution}} \bar{v}_{app,i}(\rho_{solution}) \right)} \quad (12)$$

where  $MW_i$  is the molecular weight of the sodium salt of component “i” in  $\text{g mol}^{-1}$ .

This equation is solved using the bisection method and initial guesses of 1.0 g/mL and 1.5 g/mL. The bisection method algorithm is repeated until a deviation of 0.000001 g/mL or less is observed between iterations. Once the optimized density is calculated, the weight fraction of component “i” may be calculated according to Equation (13).

$$\omega_i = \frac{[i]MW_i}{1000\rho_{solution}} \quad (13)$$

Once calculated, the mass fractions of Tank 22 are used to calculate the molarities of material exiting Tank 43.

### 3.3.4.3 Calculation of Tank 43 Molarities

The basis for calculation of Tank 43 salt component molarities is a mass balance around the 2H Evaporator system. This mass balance is displayed visually in Figure 3-10.

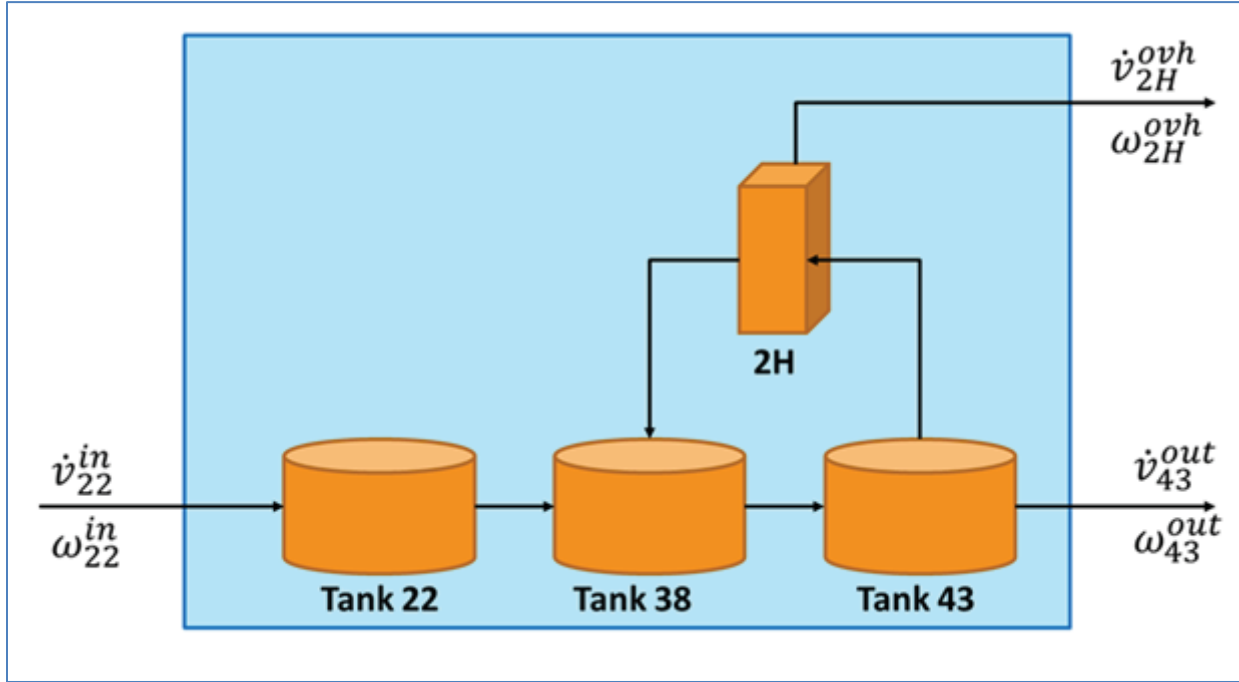


Figure 3-10. Mass Balance Around the 2H Evaporator System.

As is shown graphically in Figure 3-10, a mass balance around the 2H Evaporator system suggests that salt components enter only through Tank 22 and exit only through Tank 43 (assuming that only water is removed through the 2H Evaporator overheads). The composition of Tank 43 can then be calculated by finding the solution of the salt concentration factor,  $\theta$ , according to Equations (14) and (15).

$$\rho_f = \frac{0.001}{1 - \theta \sum_i \omega_{i,22} \frac{1}{\rho_{H_2O}} + \theta \sum_i \omega_{i,22} v_{app,i}(\theta, \omega_{i,22})} \quad (14)$$

$$\theta = \frac{\omega_{NO_2,43}}{\omega_{NO_2,22}} = \frac{\omega_{NO_3,43}}{\omega_{NO_3,22}} = \frac{\omega_{OH,43}}{\omega_{OH,22}} = \frac{\omega_{CO_3,43}}{\omega_{CO_3,22}} \quad (15)$$

The value of  $\theta$  is optimized using the bisection method and initial guesses of 1 and the maximum value achievable at an assigned solids loading limit of 75% and a completion criteria of  $<0.000001 \text{ g mL}^{-1}$  change

in density of Tank 43 material. Once the value of  $\theta$  is determined, weight fractions, density, and molarities of Tank 43 material are easily determined. It should be noted that the composition of Tank 43 material is assumed to be identical to that of Tank 38 material in this steady-state continuous flow model.

At this point, a molar concentration factor for non-degrading components (i.e., sodium salts) across the 2H Evaporator system,  $f_{Na}$ , may be derived according to Equation (16).

$$f_{Na} = \frac{[Na]_{43}}{[Na]_{22}} = \frac{[NO_2]_{43} + [NO_3]_{43} + [OH]_{43} + 2[CO_3]_{43}}{[NO_2]_{22} + [NO_3]_{22} + [OH]_{22} + 2[CO_3]_{22}} \quad (16)$$

#### 3.3.4.4 Calculation of 2H Molarities

After Tank 43 compositions have been determined, 2H Evaporator salt component molarities must be calculated to predict glycolate thermolysis in the 2H Evaporator pot. This is accomplished using a mass balance around the 2H Evaporator Pot. This mass balance is displayed graphically in Figure 3-11.

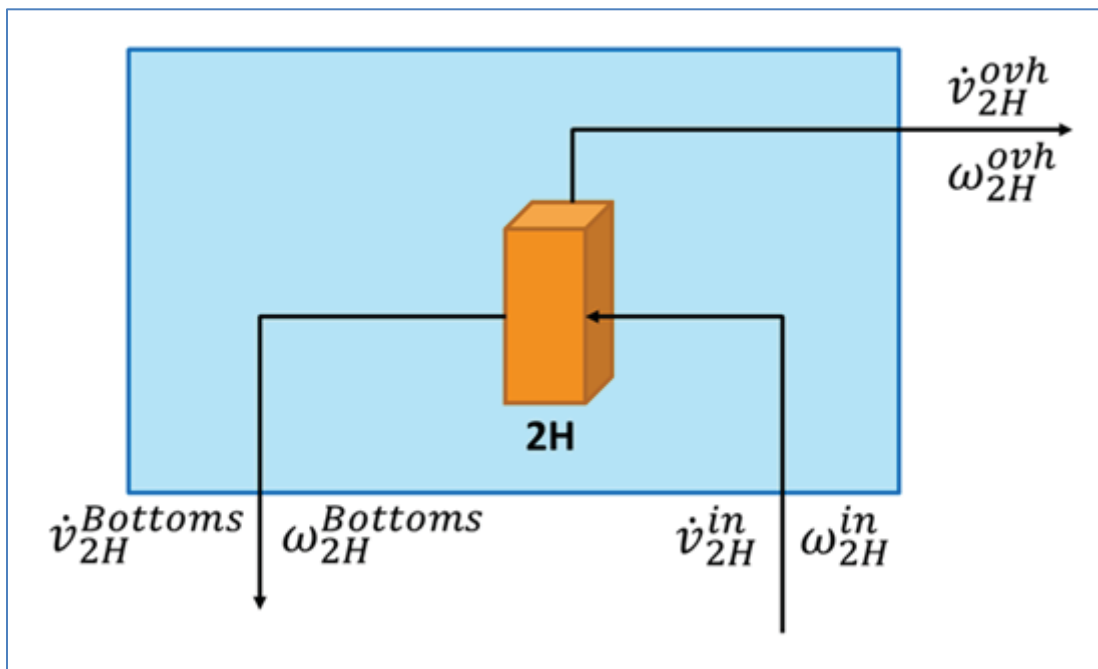


Figure 3-11. Mass Balance Around 2H Evaporator Pot.

In the mass balance illustrated in Figure 3-11, the mass flow rate of material fed to the 2H pot is calculated according to Equation (17).

$$\dot{m}_{2H}^{in} = \dot{v}_{2H}^{in} \rho_f \frac{3.785 L}{gal} \quad (17)$$

The mass flow rate of condensed overheads leaving the 2H Evaporator pot can be calculated using the total system mass balance shown in Figure 3-10. This calculation is performed using Equation (18).

$$\dot{m}_{2H}^{ovh} = \dot{v}_{22}^{in} \rho_{22} \frac{3.785 L}{gal} \left(1 - \frac{1}{\theta}\right) \quad (18)$$

The mass fractions of salt species in the 2H Evaporator pot can then be calculated according to Equation (19).

$$\omega_{i,2H} = \frac{\dot{m}_{2H}^{in}}{(\dot{m}_{2H}^{in} - \dot{m}_{2H}^{ovh})} \omega_{i,43} \quad (19)$$

Once the mass fractions in the 2H Evaporator, the density can be calculated using the Laliberte-Cooper density model and the salt component molarities can be calculated.

### 3.3.4.5 Calculation of Thermolytic Glycolate Degradation and Glycolate Concentration Factors

Once the salt concentrations in each vessel have been determined, the influence of glycolate thermolysis on the molar concentration factor of glycolate can be calculated. This calculation is accomplished by approximating the combined system (Tank 22, Tank 38, Tank 43, and the 2H Evaporator) as a system of steady-state continuously-stirred tank reactors (CSTR). For a single tank (e.g., Tank 22), the governing kinetic expression is given in Equation (20).

$$\frac{d[Gly]_{22}}{dt} = 0 = \frac{\dot{v}_{22}^{in}}{V_{22}} [Gly]_{22}^{in} - \frac{\dot{v}_{22}^{out}}{V_{22}} [Gly]_{22} - k [Gly]_{22} \quad (20)$$

where  $k$  is a tank-dependent constant derived from the non-glycolate terms (i.e., the rate constant, salt component concentrations, and the temperature-dependent Arrhenius factor) identified in Equation (3).

For the purposes of 2H system modeling, the four vessels can be described as a system of four CSTRs, corresponding to a system of four linear equations describing the glycolate kinetics in each vessel. Those equations are given in Equations (21) through (24).

$$\left(\frac{\dot{v}_{22}^{out}}{V_{22}} + k_{22}\right) [Gly]_{22} = \frac{\dot{v}_{22}^{in}}{V_{22}} [Gly]_{RCT} \quad (21)$$

$$\left(\frac{\dot{v}_{38}^{out}}{V_{38}} + k_{38}\right) [Gly]_{38} = \frac{\dot{v}_{22}^{out}}{V_{38}} [Gly]_{22} + \frac{\dot{v}_{2H}^{bottoms}}{V_{38}} [Gly]_{2H} \quad (22)$$

$$\left(\frac{\dot{v}_{43}^{out} + \dot{v}_{2H}^{in}}{V_{43}} + k_{43}\right) [Gly]_{43} = \frac{\dot{v}_{38}^{out}}{V_{43}} [Gly]_{38} \quad (23)$$

$$\left(\frac{\dot{v}_{2H}^{bottoms}}{V_{2H}} + k_{2H}\right) [Gly]_{2H} = \frac{\dot{v}_{43}^{in}}{V_{2H}} [Gly]_{43} \quad (24)$$

The system of linear equations can be rewritten in matrix format, according to Equation (25).



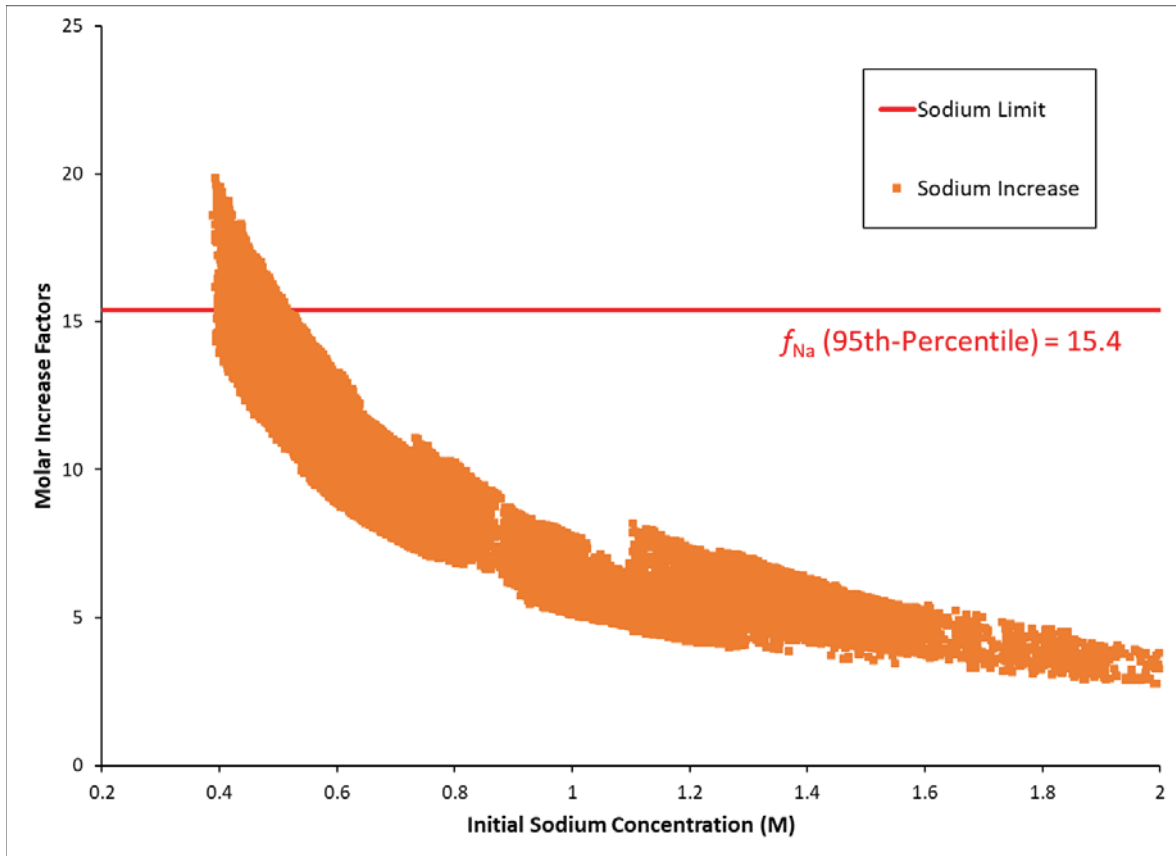
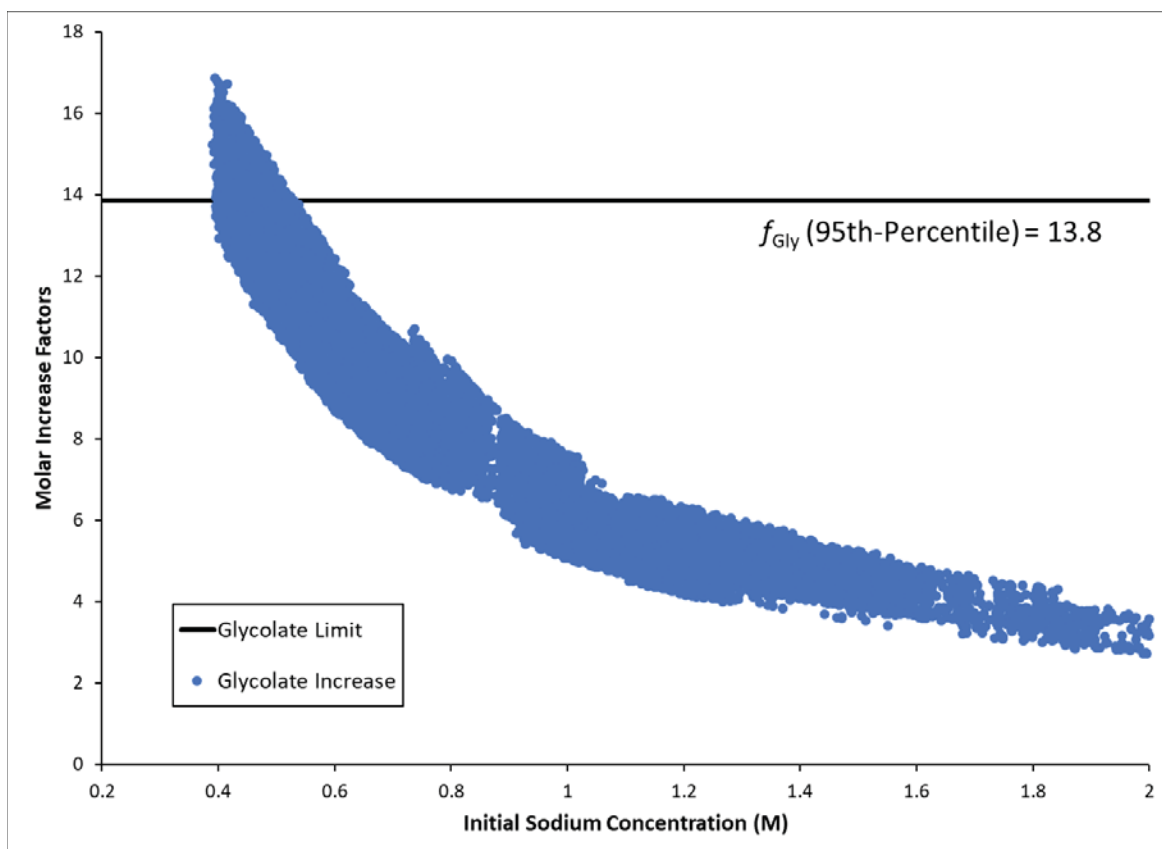


Figure 3-12. Sodium Concentration Factors Across the 2H Evaporator System Measured with 50,000 Simulations.



**Figure 3-13. Glycolate Concentration Factors Across the 2H Evaporator System Measured with 50,000 Simulations.**

The data presented in Figure 3-12 and Figure 3-13 indicate that molar concentration factors for both sodium and glycolate tend to decrease as a function of increasing initial sodium concentration (i.e., sodium concentrations in Tank 22 recycle material). This is intuitively obvious, given that a feed stream of higher sodium content would be expected to need less evaporation to achieve the same target density exiting the 2H system. Furthermore, it can be seen from the data that glycolate concentration factors tend to be slightly less than sodium concentration factors due to the ability of glycolate to thermolytically deteriorate.

As may be seen in the data given in Figure 3-13, the 95<sup>th</sup> percentile of glycolate molar concentration factors is 13.8. This suggests that 95% of possible processing options in the 2H system would be expected to lead to concentration factors of 13.8 or less. Given that processing strategies employed in 2H operation are not necessarily designed to pursue a constant density or a constant recycle stream composition, future processing of the 2H Evaporator would reasonably be expected to resemble an average of the factors displayed in Figure 3-13. Therefore, the 95<sup>th</sup> percentile value of 13.8 represents a conservatively high estimate of the most likely glycolate concentration factors to be encountered after implementation of the nitric-glycolic flowsheet. This value should be treated as a maximum multiplier for glycolate in the 2H system (e.g., if a final glycolate concentration of 5 mg L<sup>-1</sup> is expected in the RCT before transferring to Tank 22, a reasonable estimate for the maximum concentration achievable in the 2H system is 5 × 13.8 = 69 mg L<sup>-1</sup>).

#### 4.0 Conclusions and Recommendations

Two models were developed to conservatively estimate glycolate concentrations in the CSTF to alleviate potential flammability concerns due to hydrogen generation from thermolysis. To account for a glycolate source term, a model was developed to estimate residual glycolate being introduced to the CSTF via returns from DWPF. To estimate maximum glycolate concentrations in the CSTF, a model was developed to estimate concentration factors in the 2H Evaporator system and account for glycolate thermolysis in the CSTF.

A kinetic model with an additional loss term for permanganate is provided to conservatively predict P/G ratios and reaction durations required to reduce initial glycolate concentrations to a desired value in the RCT. This work indicates the following:

- Glycolate concentrations can be accurately predicted during the range of potential RCT strike and residence periods provided.
- The model can be used to predict glycolate concentration in the RCT in regions where testing is not feasible because it would lead to results below the analytical reporting limit, and
- The model predicts that an assumed glycolate content of 35 to 65 mg/L with a P/G ratio = 20 can be reduced below 1.4 mg/L in 3 hours and below 0.24 mg/L at a 6 hour residence time.

A model is provided to simulate glycolate concentration factors across the 2H Evaporator. Application of this model reveals:

- Molar concentration factors for both sodium and glycolate tend to decrease as a function of increasing initial sodium concentration, and
- 95% of processing options in the 2H system would lead to glycolate concentration factors of 13.8 or less.

It is recommended that the upcoming 3H Evaporator modeling results be incorporated with this effort to provide a final determination of potential CSTF conditions and update nitric/formic to nitric/glycolic flowsheet transition support. The calculations performed in this document should be re-evaluated in the event that DWPF RCT treatment procedures are modified.

## 5.0 References

1. D.P. Lambert, M.S. Williams, C.H. Brandenburg, M.C. Luther, J.D. Newell, and W.H. Woodham, "Sludge Batch 9 Simulant Runs Using the Nitric-Glycolic Acid Flowsheet," Savannah River National Laboratory, **SRNL-STI-2016-00319, Rev. 0**, 2016.
2. G. Chen and M. Clark, "Evaluation of Chemical Additives for Glycolate Mitigation," Savannah River Remediation, LLC, Aiken, SC, **X-TTR-S-00068, Rev. 0**, 2018.
3. D.P. Lambert, "Task Technical and Quality Assurance Plan for Evaluation of Chemical Additives for Glycolate Mitigation," Savannah River National Laboratory, Aiken, SC, **SRNL-RP-2018-00358, Rev. 0**, 2018.
4. G. Chen and E.W. Holtzscheiter, "Screening Study: Chemical Additives for Low Concentration Glycolate Decomposition in Defense Waste Processing Facility (DWPF) Recycle Stream to Tank Farm," Savannah River Remediation, LLC, Aiken, SC, **X-TAR-S-00007, Rev. 0**, 2017.
5. T.B. Peters and C.A. Nash, "Defense Waste Processing Facility (DWPF) Glycolate Mitigation: Scoping Test Results," Savannah River National Laboratory, Aiken, SC, **SRNL-L3100-2018-00043, Rev. 0**, 2018.
6. D.P. Lambert, A.M. Howe, M.S. Williams, C.L. Trivelpiece, and R.G. William, "Evaluation of Chemical Additives for Glycolate Destruction in the Recycle Collection Tank," Savannah River National Laboratory, Aiken, SC, **SRNL-STI-2018-00585, Rev. 1**, 2019.
7. J.R. Zamecnik, D.P. Lambert, W.T. Riley, and W.G. Ramsey, "Permanganate Oxidation of Defense Waste Processing Facility (DWPF) Recycle Collection Tank (RCT) Simulants – Protocol Runs for Nominal and Chemical Process Cell (CPC) Foamover Conditions," Savannah River National Laboratory, Aiken, SC, **SRNL-STI-2019-00292, Rev. 0**, 2019.
8. M.J. Siegfried, W.G. Ramsey, and M.S. Williams, "Permanganate Oxidation of Defense Waste Processing Facility (DWPF) Recycle Collection Tank (RCT) Simulants Larger Scale Protocol Runs - Chemical Process Cell (CPC) Nominal and Foamover Conditions," Savannah River National Laboratory, **SRNL-STI-2019-00588, Rev. 0**, 2019.
9. C.A. Nash and M.J. Siegfried, "Permanganate Oxidation of Actual Defense Waste Processing Facility (DWPF) Slurry Mix Evaporator Concensate Tank (SMECT) and Offgas Condensate Tank (OGCT) Samples to Remediate Glycolate," Savannah River National Laboratory, **SRNL-STI-2020-00012, Rev 0**, 2020.
10. C.J. Martino, J.M. Pareizs, and J.D. Newell, "Thermolytic Hydrogen Generation Testing of Tank 22 Material," Savannah River National Laboratory, **SRNL-STI-2018-00385, Rev. 0**, 2018.
11. W.H. Woodham and C.J. Martino, "Evaluation of Thermolytic Production of Hydrogen from Glycolate and Common Tank Farm Organics in Simulated Waste," Savannah River National Laboratory, Aiken, SC, **SRNL-STI-2019-00605, Rev. 1**, 2020.
12. JMP® Statistical Discovery Software, Professional Version 11.2.1, 64-bit, SAS Institute, Inc., Cary, NC.
13. Mathematica 12.0.0 Kernel for Microsoft Windows (64-bit) Copyright 1988-2019 Wolfram Research, Inc.
14. T.B. Edwards, "JMP Pro Version 11.2.1," **B-SWCD-W-00023, Rev. 0**, 2014.
15. S.W. Benson, "The Induction Period in Chain Reactions," *J. Chem. Phys.*, **20** 1605 (1952).
16. NTANK Tank Composition Spreadsheet Database. Savannah River Remediation.
17. M. Laliberte and W.E. Cooper, "Model for Calculating the Density of Aqueous Electrolyte Solutions," *Journal of Chemical Engineering Data*, **49** 1141-51 (2004).

## Appendix A: Glycolate analyses using OnGuard II H<sup>+</sup> and II Na<sup>+</sup> cartridges

Dionex OnGuard II cartridges are disposable pretreatment microcolumns designed to remove metals species from samples prior to analysis by Ion Chromatography (IC). Improved gaussian peak shape has been observed<sup>a</sup> when used for carboxylic acid analyses at low concentrations on a Dionex AS-11 analytical column. This approach ensures the integrated analyte peak of the sample closely matches the integrated peak of the standard used to quantify the sample.

Figure A.1 is an example of poor peak shape that is improved with the use of the cartridges. The sample is from Slurry Mixed Evaporator Condensate Tank (SMECT) radiological waste testing and contains a low concentration of glycolate. This sample<sup>b</sup> was diluted 1:10 and analyzed with and without an OnGuard II H<sup>+</sup> cartridge. The peak in the green circle is glycolate and elutes as a gaussian peak that is similar in shape to the peak in the quality control standard when the OnGuard II H<sup>+</sup> cartridge is used. Use of OnGuard II Na<sup>+</sup> cartridges did not show a significant improvement in peak shape.

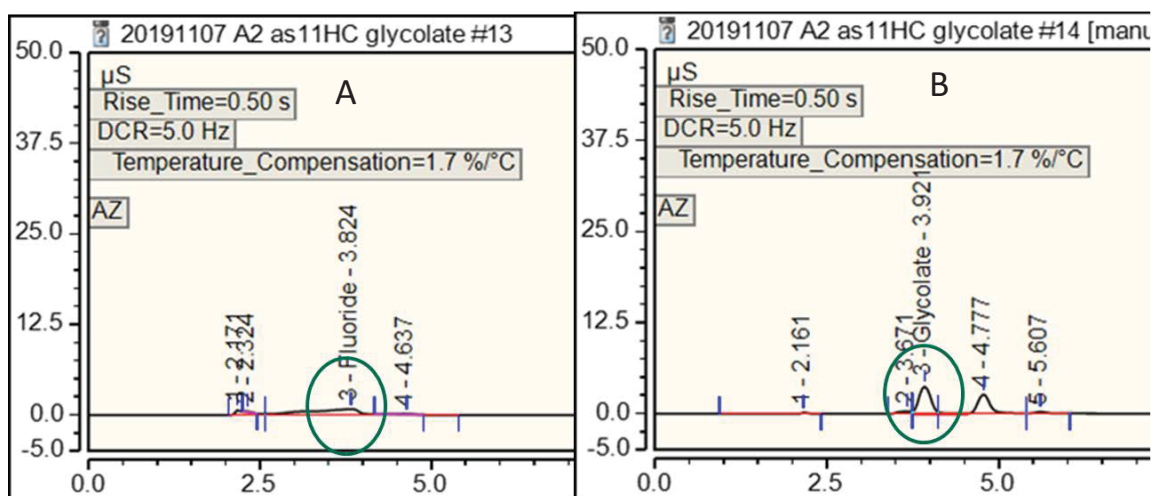


**Figure A.1:** SMECT radiological sample diluted 1:10 with deionized water without OnGuard II H<sup>+</sup> cartridge (A) and with OnGuard II H<sup>+</sup> cartridge (B) demonstrating the improved peak shape.

Some precautions need to be followed when using OnGuard II H<sup>+</sup> cartridges. The liquid that passes through the OnGuard II H<sup>+</sup> cartridge becomes contaminated with low concentrations of compounds. These compounds show a response on the IC where glycolate, formate, and sulfate elute. Using 2.5 cc cartridges, a minimum of 10 mL of sample needs to pass through the cartridge to lower the glycolate interferent to near the baseline<sup>c</sup>. Figure A-2 shows what initially elutes off the cartridge (first 5 mL of a deionized water blank) and after 15 mL of solution is eluted through the cartridge prior to collecting into a sample vial. The picture on the bottom shows glycolate and formate baseline resolved and sulfate significantly reduced in peak height. These cartridge rinses were tested on two different IC instruments (analytical 1 and analytical 2) as shown on the table.

<sup>a</sup> Kuo, C. Improved application of ion chromatographic determinations of carboxylic acids in ozonated drinking water *Journal of Chromatography A* **1998**, 804, 265-272.

<sup>b</sup> SMECT – LW-AD-PROJ-191014-3 #15665.

<sup>c</sup> White, T. L.; DiPrete, D. P.; Fondeur, F. F. *Glycolate Analysis in Tank 22: Developing and Testing Analytical Methods for the Savannah River Site Liquid Waste System*, Savannah River National Laboratory: Aiken, SC, 2020.

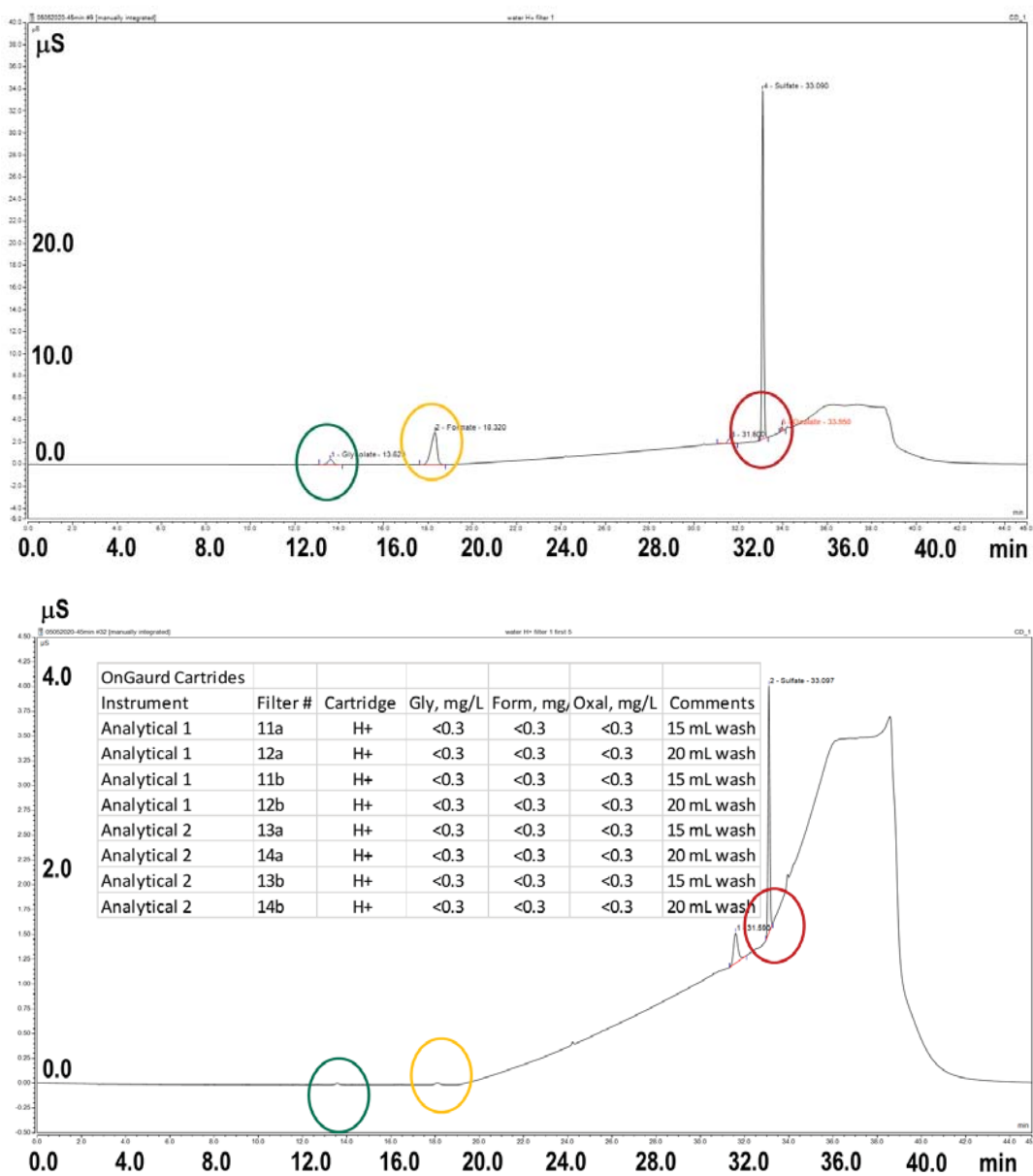


**Figure A.2: Top chromatograph shows impurities eluting off OnGuard II H<sup>+</sup> cartridge using deionized water and the bottom chromatogram shows the nearly complete loss of impurities after 15 mL of deionized water has passed through the cartridge.**

Two types of method blanks need to be analyzed when analyzing for carboxylic acids: cartridge/preparation blanks and reagent blanks to identify sources of contamination. The cartridge or preparation blanks are deionized water blanks prepared and treated in the same way as the samples and analyzed with each batch of samples. A minimum of three (n=3) should be analyzed to show any interferent consistently appears. These cartridge or preparation blank samples (n=3) should be assessed along with the reagent blank (deionized water used for dilutions) to ensure interferences from contaminants are not occurring. Applying blank subtraction to sample results data becomes more important when sample volume is limited (<20 mL) which often occurs for radioactive samples and when low concentrations of glycolate (10-50 mg/L) need to be quantified. To do so, use Equation A-1 where the sample concentration is subtracted from the average

of the cartridge/preparation concentration. In our work on radiological samples cartridge/preparation blanks were subtracted from a sample results to give cartridge blank subtracted results that matched expected values<sup>3</sup>.

$$\text{Sample concentration} - \text{Cartridge blank concentration} = \text{Cartridge blank subtracted result} \quad (\text{A-1})$$

Testing at the Process Science Analytical Laboratory (PSAL) also showed contamination from OnGuard II H<sup>+</sup> cartridges on their two anion chromatography instruments. OnGuard II 2.5 cc H<sup>+</sup> and Na<sup>+</sup> cartridges were tested by passing 5 mL of deionized water through and analyzing on both instruments. Table A.1 shows that the H<sup>+</sup> cartridge had consistent IC responses where Glycolate and Formate elute. The average of five cartridge blank concentration values for glycolate and formate shown in the red circle were used to account for cartridge contamination in the IC samples used in this report (Equation A-1).

**Table A.1: OnGuard II test for contaminants**

H+ cartridge			
#	Gly, mg/L	Form, mg/L	Oxal, mg/L
1	1.00435	4.74295	0.4169
2	1.02105	4.70175	0.39905
3	1.0261	4.5361	0.3899
4	1.0021	4.4633	0.2219
5	1.0235	4.48615	0.22295
Average	1.02	4.59	0.330
stdev	0.0113	0.128	0.0988
%rsd	1.11	2.79	29.9
Na+ cartridge			
#	Gly, mg/L	Form, mg/L	Oxal, mg/L
1	<0.3	<0.3	<0.3
2	<0.3	<0.3	<0.3
3	<0.3	<0.3	<0.3
4	<0.3	<0.3	<0.3
5	<0.3	<0.3	<0.3

## Appendix B: Statistical Development of the Empirical Reaction Model

While the kinetic reaction model with loss term is not tractable by JMP® Pro, Ver. 11.2.1, the body of simulant and radioactive waste sample test data was used with JMP® to form an empirical model for providing statistical predictions. Since empirical model terms are not constrained by mechanistic reasoning, best judgement was used to select terms, and JMP® was used to verify their relevance for fitting the experimental data. The empirical model is referred to as the “regression fit” in the main report. As such, it was only used with JMP and is not used for glycolate predictions below practical reporting limits.

The terms of the resulting model were used to predicted G (mM) as a function of the intercept, a term using  $G(0) * a / (t + a)$  where “t” is the experimental time in minutes, “a” is a constant to be estimated, and is the inverse of P/G ( $a = G/P$ ). The non-linear estimation routine in JMP® was used to estimate the value of “a” in the empirical model that has a root mean square of 0.020 mM. Details on the model fit and performance of the model are shown in Exhibit 1.

Exhibit 2 then uses this term plus an intercept term and the inverse of P/G to obtain the empirical model for predicting G (mM). This model is only valid in the region of the experimental database for initial G (0.85 to 2.439 mM), P/G (1.88 to 15.1) as shown in Figure B.1, and reaction times ranging from 0 to 180 minutes.

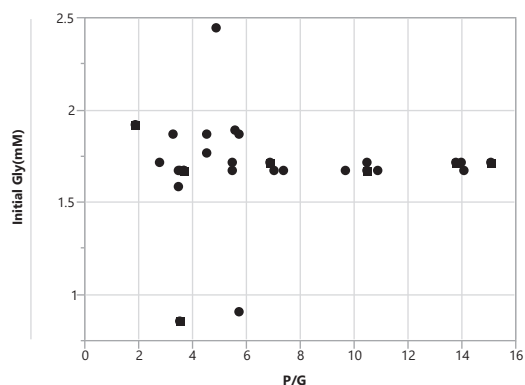


**Figure B.1**

The empirical model is the best estimate representation of the database and provides predictions for G (mM) with a root mean square of 0.12 mM used in developing 95% confidence bounds for individual predictions.

Exhibit 3 compares the empirical model to the theoretical model with reaction rate constants  $K_1$  and  $K_x$  from the SMECT experiment (nonlinear least squares) to show how the theoretical model bounds the body of experimental data. The theoretical model, evaluated using the numerical integration function NIntegrate in Mathematica Ver. 12.0.0, fits the SMECT data with rate constants  $K_1 = 0.00286$  1/min/mM and  $K_x = 0.00276$  1/min. This model is shown to conservatively bound 88.7% of the data (single point) and 84.2% of the test data population (complete calculation through time) with 95% confidence. The theoretical model is thus conservative and is reasonably expected to predict a higher G (mM) on average than would be seen in a batch reaction. It was developed to be used both within the experimental range of data as well as for a conservative extrapolation to G lower than can be measured by experiment.

Exhibit 4 is simply a set of 95 uses of the theoretical model, one run per experimental point, to help provide the comparison showing how conservative the theoretical model is with respect to measured batch reaction

# Exhibit 1

## Non-Linear Empirical Model based on SMECT Data

### Nonlinear Fit

Prediction Model:  $g(x)=$

$$\frac{\left( \text{Initial Gly(mM)} \quad * \quad a \right)}{\left( a + \text{ExpTime (min)} \right)}$$

Response: Glycolate(mM), JMP® Pro, Ver. 11.2.1 is used to estimate “a”

Criterion	Current	Stop Limit
Iteration	2	9999999
Obj Change	3.7530721e-9	1e-15
Relative Gradient	1.2004442e-6	0.000001
Gradient	1.5906446e-8	0.000001

Parameter	Current Value
a	27.156814905

### Solution

SSE	DFE	MSE	RMSE
0.0016442401	4	0.0004111	0.0202746

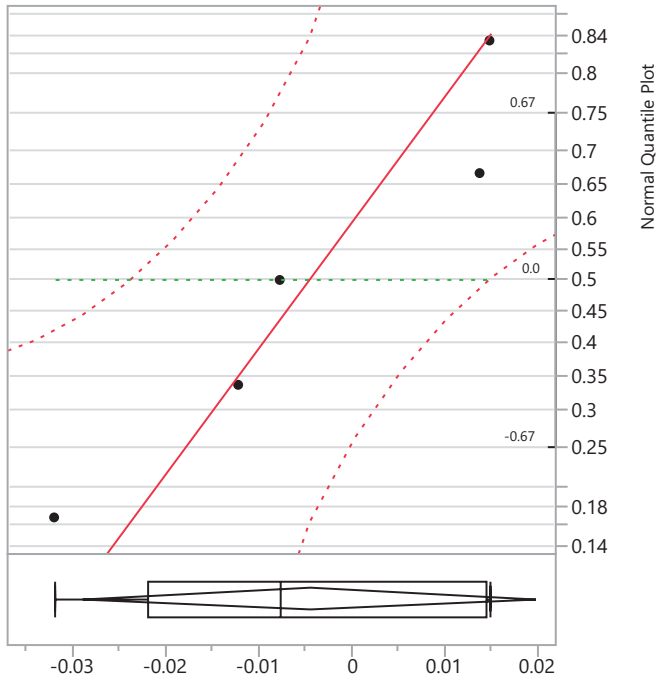
Parameter	Estimate	ApproxStdErr	Lower CL	Upper CL
a	27.156814905	0.68428409	25.3068828	29.0906241

Solved By: Analytic Gauss-Newton

### Non-Linear Regression Terms

Term	Abbreviated Description	Full Description
SSE	Sum of Squares for Error	SSE shows the residual sum of squares error. SSE is the objective that is to be minimized.
DFE	Degrees of Freedom for SSE	DFE is the degrees of freedom for error, which is the number of observations used minus the number of parameters fitted.
MSE	Mean Square Error	MSE shows the mean squared error. It is the estimate of the variance of the residual error, which is the SSE divided by the DFE.
RMSE	Root Mean Square Error	RMSE estimates the standard deviation of the residual error, which is square root of the MSE.
ApproxStdErr	Approximate Standard Error of the Estimate	ApproxStdErr lists the approximate standard error.
Lower CL	Lower Confidence Limit for the Estimate	[Lower CL, Upper CL]: 95% Confidence Interval for the Estimate.
Upper CL	Upper Confidence Limit for the Estimate	[Lower CL, Upper CL]: 95% Confidence Interval for the Estimate.

**Distribution:  
Residuals for the g(x) Non-Linear Model**



**Quantiles**

100.0%	maximum	0.01509
75.0%	quartile	0.01455
50.0%	median	-0.0077
25.0%	quartile	-0.022
0.0%	minimum	-0.0318

**Summary Statistics**

Mean	-0.004506
Std Dev	0.0196386
Std Err Mean	0.0087827
Upper 95% Mean	0.0198781
Lower 95% Mean	-0.028891
N	5

**Fitted Normal Parameter Estimates**

Type	Parameter	Estimate	Lower 95%	Upper 95%
Location	$\mu$	-0.004506	-0.028891	0.0198781
Dispersion	$\sigma$	0.0196386	0.0117661	0.0564326

**Goodness-of-Fit Test**

Shapiro-Wilk W Test

**W**                      **Prob<W**  
0.911888                0.4790

Note: Ho = The data is from the Normal distribution. Small p-values reject Ho.

**Data and Statistical Results for SMECT Non-Linear Empirical Model**

ID	Test #	Initial Gly (mM)	P/G	Glycolate (mM)	Theo Time (min)	ExpTime (min)	Time Diff (Theo-Exp) (min)	Glycolate2 (mg/L)
1	SMECT	1.932	5.6	0.342	118.43	121	-2.57	25.7
2	SMECT	1.932	5.6	0.429	92.5	93	-0.5	32.2
3	SMECT	1.932	5.6	0.616	59.69	60	-0.31	46.3
4	SMECT	1.932	5.6	0.902	33.73	32	1.73	67.7
5	SMECT	1.932	5.6	0.219	186.84	182	4.84	16.4

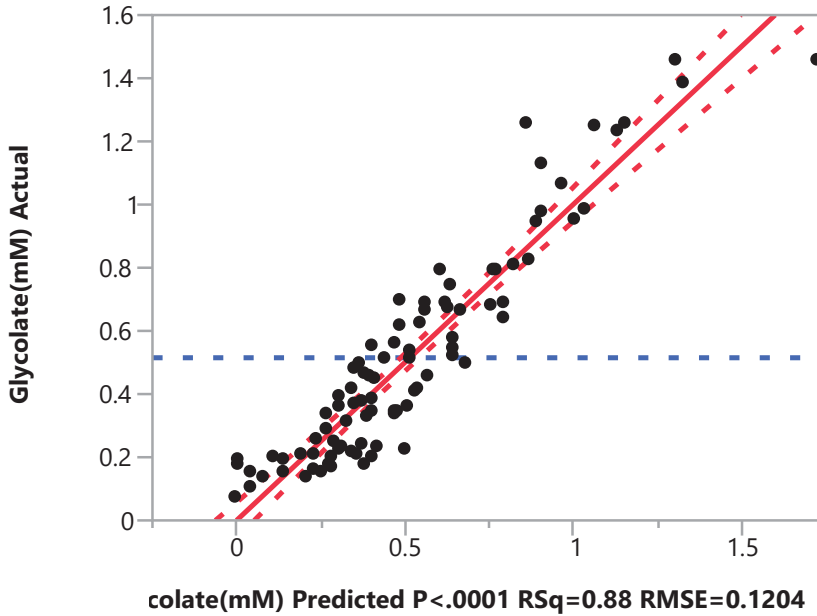
ID	g(x) NL Mod (mM)	Fitted g(x) NL Mod (mM)	StdError Fitted g(x) NL Mod (mM)	StdError Indiv g(x) NL Mod (mM)
1	0.015836	0.354131	0.007288	0.021545
2	0.020553	0.436654	0.008516	0.021990
3	0.031672	0.601984	0.010442	0.022806
4	0.058545	0.886913	0.012089	0.023605
5	0.010557	0.250850	0.005500	0.021007

ID	LowerM g(x) NL Mod (mM)	UpperM g(x) NL Mod (mM)	LowerI g(x) NL Mod (mM)	UpperI g(x) NL Mod (mM)	Residuals g(x) NL Mod (mM)	Pred % err
1	0.333898	0.374365	0.294314	0.413949	-0.012131	-3.55
2	0.413010	0.460298	0.375599	0.497709	-0.007654	-1.78
3	0.572991	0.630976	0.538665	0.665302	0.014016	2.28
4	0.853349	0.920477	0.821375	0.952452	0.015087	1.67
5	0.235579	0.266121	0.192524	0.309176	-0.031850	-14.54

# Exhibit 2

## Empirical Model from Experimental Data

Response Glycolate(mM)  
Actual by Predicted Plot



Dotted Red Lines represent the lower and upper 95% confidence limits for the mean response.

### Summary of Fit

RSquare	0.878933
RSquare Adj	0.87615
Root Mean Square Error	0.120362
Mean of Response	0.514967
Observations	90

### Analysis of Variance

Source	DF	Sum of Squares	Mean Square	F Ratio
Model	2	9.150069	4.57503	315.8050
Error	87	1.260360	0.01449	<b>Prob &gt; F</b>
C. Total	89	10.410429		<.0001*

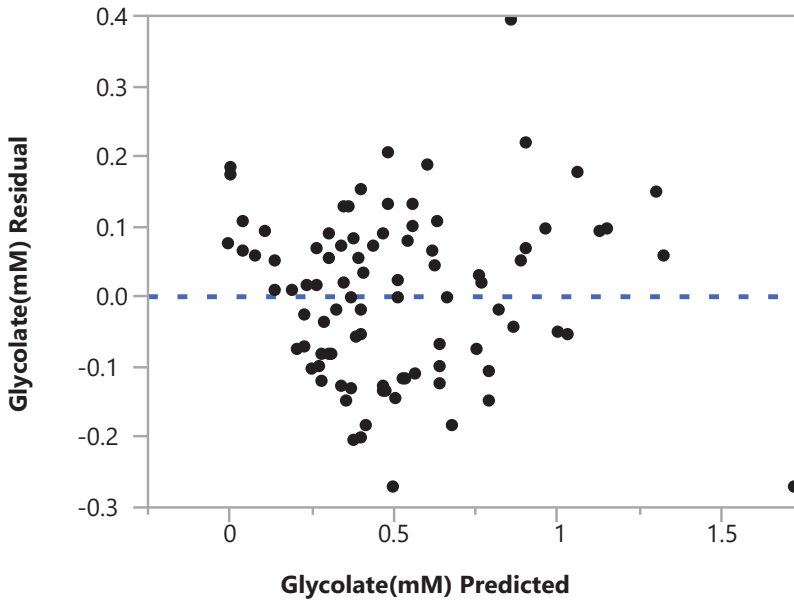
DF: Degrees of Freedom

C. Total: Total Sum of Squares corrected for the Mean

### Parameter Estimates

Term	Estimate	Std Error	t Ratio	Prob> t
Intercept	-0.609319	0.0465	-13.10	<.0001*
g(x)	0.8642859	0.046435	18.61	<.0001*
G/P	2.915997	0.139744	20.87	<.0001*

**Residual by Predicted Plot**



**Correlation of Estimates**

Corr	Intercept	g(x)	G/P
Intercept	1.0000	-0.7111	-0.7999
g(x)	-0.7111	1.0000	0.2404
G/P	-0.7999	0.2404	1.0000

where

g(x)=

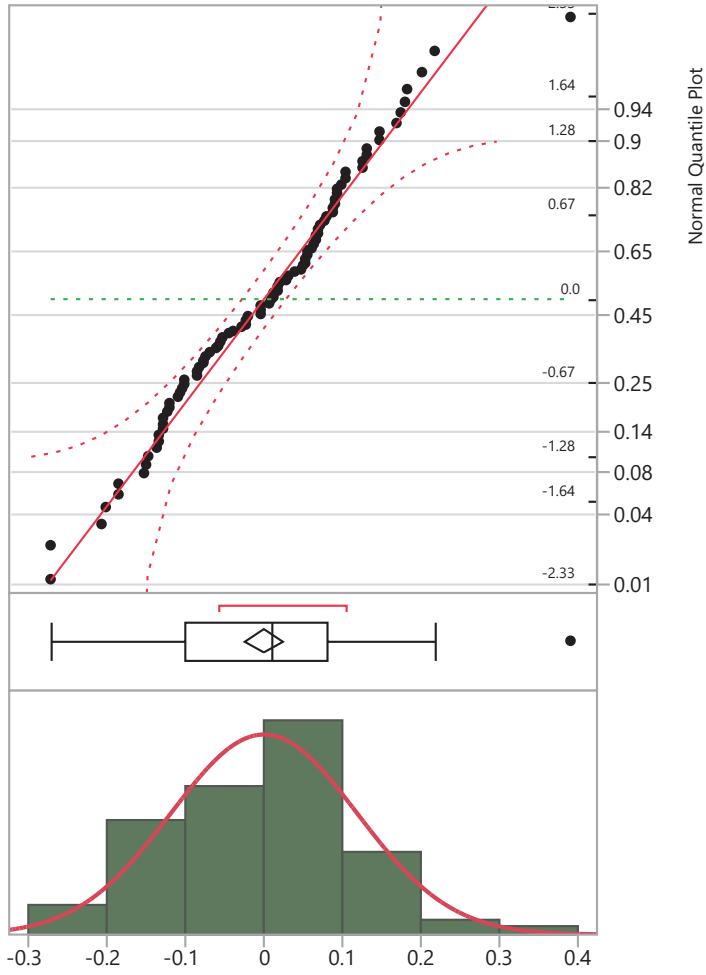
$$\frac{\text{Initial Gly}(mM) * 27.1568149046421}{27.1568149046421 + \text{ExpTime} (min)}$$

is based on the SMECT data (N=5). Exhibit 1

**Predicted Glycolate(mM)=**

$$-0.6093194685421 + 0.86428590528871 * \left( \frac{\text{Initial Gly}(mM) * 27.1568149046421}{27.1568149046421 + \text{ExpTime} (min)} \right) + 2.91599703119392 * G/P$$

**Distributions Residual Glycolate(mM)**



**Quantiles**

100.0%	maximum	0.39194
75.0%	quartile	0.08231
50.0%	median	0.01175
25.0%	quartile	-0.0995
0.0%	minimum	-0.2728

**Summary Statistics**

Mean	-7.31e-17
Std Dev	0.1190015
Std Err Mean	0.0125439
Upper 95% Mean	0.0249244
Lower 95% Mean	-0.024924
N	90

**Fitted Normal****Parameter Estimates**

Type	Parameter	Estimate	Lower 95%	Upper 95%
Location	$\mu$	-7.31e-17	-0.024924	0.0249244
Dispersion	$\sigma$	0.1190015	0.1037946	0.1394704

**Goodness-of-Fit Test**

Shapiro-Wilk W Test

W	Prob<W
0.983571	0.3159

Note: Ho = The data is from the Normal distribution. Small p-values reject Ho.

**Data for the Regression, Predictions and 95% Confidence Limits for Individual Predictions**

Test #	G0 (mM)	P/G	G (mM)	ExpTime (min)	g(x)	Pred G (mM)	Lower 95% Indiv G (mM)	Upper 95% Indiv G (mM)	Residual G (mM)
	1.666	9.72	0.372	30	0.79156	0.37482	0.13171	0.61793	-0.00282
1	1.866	3.32	1.456	15	1.20205	1.30791	1.05773	1.55809	0.14809
1	1.866	3.32	0.98	30	0.88659	1.03526	0.79106	1.27946	-0.05526
1	1.866	3.32	0.795	61	0.57482	0.76580	0.52419	1.00742	0.02920
1	1.866	3.32	0.574	90	0.43254	0.64283	0.40126	0.88440	-0.06883
1	1.866	3.32	0.457	120	0.34436	0.56662	0.32472	0.80851	-0.10962
1	1.866	3.32	0.345	180	0.24462	0.48041	0.23782	0.72301	-0.13541
2	1.866	4.57	1.245	15	1.20205	1.06767	0.81978	1.31556	0.17733
2	1.866	4.57	0.689	30	0.88659	0.79502	0.55251	1.03753	-0.10602
2	1.866	4.57	0.412	60	0.58142	0.53127	0.29069	0.77184	-0.11927
2	1.866	4.57	0.346	90	0.43254	0.40259	0.16177	0.64341	-0.05659
2	1.866	4.57	0.308	120	0.34436	0.32638	0.08504	0.56771	-0.01838
2	1.866	4.57	0.254	180	0.24462	0.24018	-0.00207	0.48242	0.01382
3	1.714	13.8	0.395	30	0.81437	0.30583	0.06150	0.55017	0.08917
3	1.866	5.74	0.806	20	1.07460	0.82745	0.58237	1.07254	-0.02145
3	1.866	5.74	0.661	30	0.88659	0.66496	0.42247	0.90746	-0.00396
3	1.866	5.74	0.38	60	0.58142	0.40121	0.16030	0.64211	-0.02121
3	1.866	5.74	0.287	90	0.43254	0.27253	0.03121	0.51385	0.01447
3	1.866	5.74	0.205	120	0.34436	0.19632	-0.04562	0.43825	0.00868
3	1.866	5.74	0.201	182	0.24228	0.10809	-0.13489	0.35108	0.09291
4	1.714	13.8	0.222	30	0.81437	0.30583	0.06150	0.55017	-0.08383
6	1.666	14.1	0.197	30	0.79156	0.28163	0.03734	0.52591	-0.08463
7	0.85	3.55	0.74	20	0.48950	0.63516	0.39406	0.87626	0.10484
7	0.85	3.55	0.661	30	0.40386	0.56114	0.31985	0.80242	0.09986
7	0.85	3.55	0.51	61	0.26184	0.43840	0.19623	0.68056	0.07160
7	0.85	3.55	0.461	91	0.19536	0.38094	0.13812	0.62375	0.08006
7	0.85	3.55	0.417	120	0.15686	0.34766	0.10440	0.59093	0.06934
7	0.85	3.55	0.363	181	0.11089	0.30793	0.06406	0.55180	0.05507
9	1.714	15.1	0.25	30	0.81437	0.28764	0.04305	0.53224	-0.03764
9	1.714	15.1	0.152	60	0.53406	0.04537	-0.19912	0.28987	0.10663
11a	1.666	7.06	0.62	30	0.79156	0.48785	0.24573	0.72996	0.13215
12	1.582	3.51	0.956	20	0.91105	1.00885	0.76482	1.25289	-0.05285
12	1.582	3.51	0.827	30	0.75165	0.87109	0.62888	1.11331	-0.04409
12	1.582	3.51	0.521	60	0.49293	0.64748	0.40633	0.88863	-0.12648
12	1.582	3.51	0.419	90	0.36671	0.53839	0.29689	0.77988	-0.11939
12	1.582	3.51	0.346	120	0.29195	0.47378	0.23182	0.71573	-0.12778

Test #	G0 (mM)	P/G	G (mM)	ExpTime (min)	g(x)	Pred G (mM)	Lower 95% Indiv G (mM)	Upper 95% Indiv G (mM)	Residual G (mM)
12	1.582	3.51	0.2	180	0.20739	0.40069	0.15797	0.64341	-0.20069
12a	1.666	3.55	0.947	30	0.79156	0.89623	0.65372	1.13873	0.05077
12a	1.666	3.55	0.624	90	0.38618	0.54586	0.30450	0.78721	0.07814
12a	1.666	3.55	0.551	180	0.21840	0.40085	0.15828	0.64342	0.15015
12a	1.666	3.55	0.329	195	0.20365	0.38810	0.14538	0.63083	-0.05910
13	1.666	9.72	0.149	60	0.51910	0.13933	-0.10361	0.38227	0.00967
13	1.764	4.55	0.978	20	1.01586	0.90955	0.66523	1.15387	0.06845
13	1.764	4.55	0.681	30	0.83813	0.75594	0.51395	0.99793	-0.07494
13	1.764	4.55	0.361	60	0.54964	0.50660	0.26604	0.74716	-0.14560
13	1.764	4.55	0.179	90	0.40889	0.38496	0.14403	0.62589	-0.20596
13	1.764	4.55	0.231	120	0.32553	0.31291	0.07144	0.55439	-0.08191
13	1.764	4.55	0.158	180	0.23125	0.23142	-0.01096	0.47381	-0.07342
14	1.886	5.62	0.643	23	1.02115	0.79211	0.54789	1.03633	-0.14911
14	1.886	5.62	0.499	30	0.89609	0.68402	0.44145	0.92660	-0.18502
14	1.886	5.62	0.233	60	0.58765	0.41744	0.17659	0.65829	-0.18444
14	1.886	5.62	0.166	90	0.43717	0.28738	0.04615	0.52861	-0.12138
14	1.886	5.62	0.133	120	0.34805	0.21035	-0.03147	0.45218	-0.07735
14a	1.666	7.38	0.559	30	0.79156	0.46994	0.22770	0.71218	0.08906
14a	1.666	7.38	0.208	60	0.51910	0.23445	-0.00739	0.47630	-0.02645
15a	1.919	1.88	1.457	30	0.91177	1.72977	1.46948	1.99007	-0.27277
15a	1.919	1.88	1.384	90	0.44482	1.32620	1.07132	1.58107	0.05780
15a	1.919	1.88	1.254	180	0.25157	1.15917	0.90443	1.41391	0.09483
16a	1.666	5.49	0.791	30	0.79156	0.60596	0.36438	0.84755	0.18504
16a	1.666	5.49	0.151	90	0.38618	0.25559	0.01413	0.49706	-0.10459
21	1.714	6.89	0.514	30	0.81437	0.51775	0.27554	0.75996	-0.00375
21	1.714	6.89	0.176	60	0.53406	0.27548	0.03394	0.51703	-0.09948
21	1.714	6.89	0.19	180	0.22469	0.00810	-0.23592	0.25212	0.18190
22	1.714	10.5	0.239	30	0.81437	0.37224	0.12875	0.61573	-0.13324
25	1.714	2.8	1.228	30	0.81437	1.13596	0.89039	1.38152	0.09204
25	1.714	2.8	0.794	90	0.39730	0.77549	0.53214	1.01884	0.01851
25	1.714	2.8	0.668	180	0.22469	0.62631	0.38209	0.87052	0.04169
26	1.714	5.5	0.689	30	0.81437	0.62471	0.38294	0.86648	0.06429
27	1.714	14	0.205	26	0.87565	0.35578	0.11101	0.60055	-0.15078
28	1.666	7.04	0.693	30	0.79156	0.48902	0.24691	0.73113	0.20398
29	1.666	10.5	0.48	30	0.79156	0.35253	0.10917	0.59589	0.12747
29	1.666	10.5	0.174	90	0.38618	0.00216	-0.24197	0.24629	0.17184
30	1.666	3.69	1.257	30	0.79156	0.86506	0.62280	1.10732	0.39194
30	1.666	3.69	0.537	90	0.38618	0.51469	0.27348	0.75591	0.02231

Test #	G0 (mM)	P/G	G (mM)	ExpTime (min)	g(x)	Pred G (mM)	Lower 95% Indiv G (mM)	Upper 95% Indiv G (mM)	Residual G (mM)
30	1.666	3.69	0.226	96	0.36736	0.49843	0.25712	0.73974	-0.27243
30	1.666	3.69	0.497	180	0.21840	0.36968	0.12721	0.61216	0.12732
7a	0.906	5.76	0.368	20	0.52175	0.34787	0.10688	0.58886	0.02013
7a	0.906	5.76	0.336	30	0.43047	0.26898	0.02763	0.51032	0.06702
7a	0.906	5.76	0.19	60	0.28230	0.14092	-0.10163	0.38346	0.04908
7a	0.906	5.76	0.135	90	0.21001	0.07844	-0.16497	0.32184	0.05656
7a	0.906	5.76	0.104	120	0.16720	0.04144	-0.20257	0.28544	0.06256
7a	0.906	5.76	0.072	181	0.11820	-0.00091	-0.24567	0.24385	0.07291
7a	1.666	3.49	1.129	30	0.79156	0.91035	0.66772	1.15298	0.21865
7a	1.666	3.49	0.692	90	0.38618	0.55998	0.31855	0.80141	0.13202
7a	1.666	3.49	0.446	180	0.21840	0.41497	0.17234	0.65760	0.03103
7a	1.666	3.49	0.454	199	0.20005	0.39911	0.15629	0.64193	0.05489
8a	1.666	10.9	0.215	30	0.79156	0.34234	0.09886	0.58582	-0.12734
OGCT	2.439	4.9	1.064	31	1.13891	0.97013	0.72375	1.21651	0.09387
OGCT	2.439	4.9	0.543	60	0.75996	0.64260	0.40132	0.88388	-0.09960
OGCT	2.439	4.9	0.336	91	0.56057	0.47028	0.22967	0.71088	-0.13428
SMECT	1.932	5.6	0.902	32	0.88691	0.67794	0.43547	0.92041	0.22406
SMECT	1.932	5.6	0.616	60	0.60198	0.43168	0.19083	0.67253	0.18432
SMECT	1.932	5.6	0.429	93	0.43665	0.28879	0.04757	0.53001	0.14021
SMECT	1.932	5.6	0.342	121	0.35413	0.21746	-0.02430	0.45923	0.12454
SMECT	1.932	5.6	0.219	182	0.25085	0.12820	-0.11459	0.37099	0.09080

# Exhibit 3

## Mathematica Evaluation of the Theoretical Upper G (mM) Limit

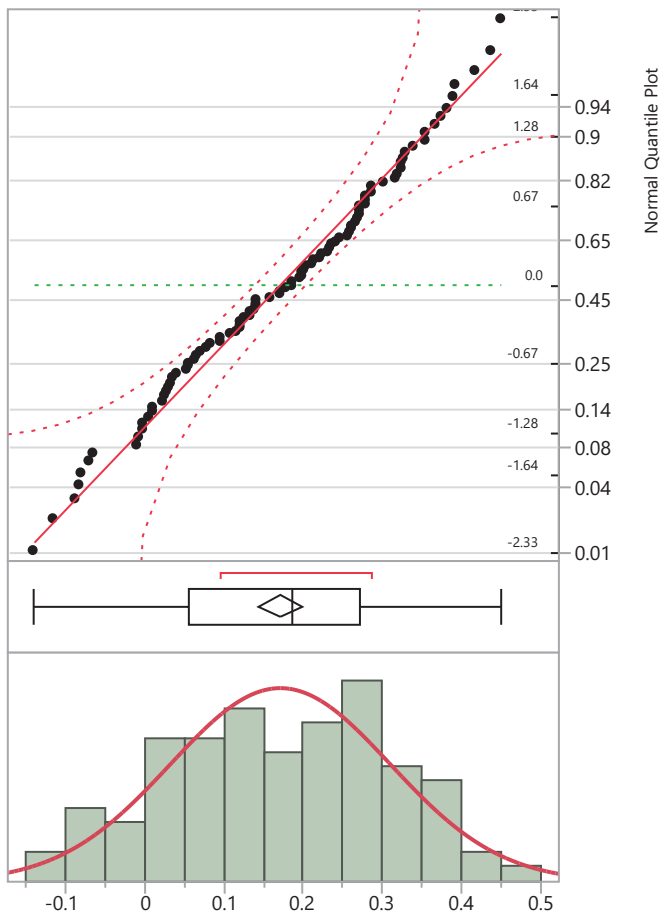
$$Time(min) = -\int_{G_0}^{G_1} \left\{ k_1 x \left[ (P_0 + 4x - 4G_0) + (k_2 / k_1) \ln(x / G_0) \right] \right\}^{-1} dx$$

$$k_1 = 0.00286, k_2 = 0.00276$$

Using Mathematica NIntegrate (numerical integration) version 12.0.0

### Distributions

#### Theo G- Expt G (mM)



### Quantiles

100.0%	maximum	0.451
75.0%	quartile	0.272
50.0%	median	0.187
25.0%	quartile	0.056
0.0%	minimum	-0.14

## Summary Statistics

Mean	0.1711895
Std Dev	0.1392772
Std Err Mean	0.0142895
Upper 95% Mean	0.1995617
Lower 95% Mean	0.1428173
N	95

## Fitted Normal

### Parameter Estimates

Type	Parameter	Estimate	Lower 95%	Upper 95%
Location	$\mu$	0.1711895	0.1428173	0.1995617
Dispersion	$\sigma$	0.1392772	0.1218975	0.1624825

## Goodness-of-Fit Test

Shapiro-Wilk W Test

W	Prob<W
0.982728	0.2449

Note: Ho = The data is from the Normal distribution. Small p-values reject Ho.

## Confidence Intervals

Parameter	Estimate	Lower CI	Upper CI	1-Alpha
Mean	0.171189	0.142817	0.199562	0.950
Std Dev	0.139277	0.121898	0.162482	0.950

## One-sided Prediction Interval

*Lower 88.7% Prediction Limit is approx. 0 (Theo G > Expt G)*

Parameter	Future N	Lower PI	Upper PI	1-Alpha
Individual	1	0.000558	.	0.887

## One-sided Tolerance Interval

*Lower Tolerance Limit for 84.2% of the Population with 95% Confidence is approx. 0*

Proportion	Lower TI	Upper TI	1-Alpha
0.842	-1.41e-6	.	0.950

## Exhibit 4

### Mathematica Evaluation of the Theoretical Upper G (mM) Limit vs. the Experimental G (mM)

Row	Test #	G0 (mM)	P/G	Expt G (mM)	Theo G (mM)	Time (min)	Theo G- Expt G (mM)
1	1	1.866	3.32	1.456	1.49	15	0.034
2	1	1.866	3.32	0.98	1.26	30	0.28
3	1	1.866	3.32	0.795	0.994	61	0.199
4	1	1.866	3.32	0.574	0.861	90	0.287
5	1	1.866	3.32	0.457	0.777	120	0.32
6	1	1.866	3.32	0.345	0.686	180	0.341
7	2	1.866	4.57	1.245	1.365	15	0.12
8	2	1.866	4.57	0.689	1.08	30	0.391
9	2	1.866	4.57	0.412	0.768	60	0.356
10	2	1.866	4.57	0.346	0.604	90	0.258
11	2	1.866	4.57	0.308	0.505	120	0.197
12	2	1.866	4.57	0.254	0.394	180	0.14
13	3	1.714	13.8	0.395	0.33	30	-0.065
14	3	1.866	5.74	0.806	1.131	20	0.325
15	3	1.866	5.74	0.661	0.93	30	0.269
16	3	1.866	5.74	0.38	0.591	60	0.211
17	3	1.866	5.74	0.287	0.421	90	0.134
18	3	1.866	5.74	0.205	0.321	120	0.116
19	3	1.866	5.74	0.201	0.211	182	0.01
20	4	1.714	13.8	0.222	0.33	30	0.108
21	6	1.666	14.1	0.197	0.324	30	0.127
22	7	0.85	3.55	0.74	0.729	20	-0.011
23	7	0.85	3.55	0.661	0.684	30	0.023
24	7	0.85	3.55	0.51	0.581	61	0.071
25	7	0.85	3.55	0.461	0.516	91	0.055
26	7	0.85	3.55	0.417	0.473	120	0.056
27	7	0.85	3.55	0.363	0.415	181	0.052
28	9	1.714	15.1	0.25	0.28	30	0.03
29	9	1.714	15.1	0.152	0.064	60	-0.088
30	12	1.582	3.51	0.956	1.215	20	0.259
31	12	1.582	3.51	0.827	1.098	30	0.271
32	12	1.582	3.51	0.521	0.875	60	0.354
33	12	1.582	3.51	0.419	0.749	90	0.33
34	12	1.582	3.51	0.346	0.672	120	0.326
35	12	1.582	3.51	0.2	0.582	180	0.382
36	13	1.666	9.72	0.149	0.244	60	0.095

Row	Test #	G0 (mM)	P/G	Expt G (mM)	Theo G (mM)	Time (min)	Theo G- Expt G (mM)
37	13	1.764	4.55	0.978	1.21	20	0.232
38	13	1.764	4.55	0.681	1.048	30	0.367
39	13	1.764	4.55	0.361	0.755	60	0.394
40	13	1.764	4.55	0.179	0.598	90	0.419
41	13	1.764	4.55	0.231	0.503	120	0.272
42	13	1.764	4.55	0.158	0.395	180	0.237
43	14	1.886	5.62	0.643	1.08	23	0.437
44	14	1.886	5.62	0.499	0.95	30	0.451
45	14	1.886	5.62	0.233	0.609	60	0.376
46	14	1.886	5.62	0.166	0.437	90	0.271
47	14	1.886	5.62	0.133	0.337	120	0.204
48	21	1.714	6.89	0.514	0.781	30	0.267
49	21	1.714	6.89	0.176	0.455	60	0.279
50	21	1.714	6.89	0.19	0.12	180	-0.07
51	22	1.714	10.5	0.239	0.502	30	0.263
52	25	1.714	2.8	1.228	1.26	30	0.032
53	25	1.714	2.8	0.794	0.934	90	0.14
54	25	1.714	2.8	0.668	0.79	180	0.122
55	26	1.714	5.5	0.689	0.922	30	0.233
56	27	1.714	14	0.205	0.392	26	0.187
57	28	1.666	7.04	0.693	0.759	30	0.066
58	29	1.666	10.5	0.48	0.504	30	0.024
59	29	1.666	10.5	0.174	0.094	90	-0.08
60	30	1.666	3.69	1.257	1.117	30	-0.14
61	30	1.666	3.69	0.537	0.736	90	0.199
62	30	1.666	3.69	0.226	0.544	196	0.318
63	30	1.666	3.69	0.497	0.559	180	0.062
64	11a	1.666	7.06	0.62	0.76	30	0.14
65	12a	1.666	3.55	0.947	1.134	30	0.187
66	12a	1.666	3.55	0.624	0.763	90	0.139
67	12a	1.666	3.55	0.551	0.591	180	0.04
68	12a	1.666	3.55	0.329	0.577	195	0.248
69	14a	1.666	7.38	0.559	0.73	30	0.171
70	14a	1.666	7.38	0.208	0.41	60	0.202
71	15a	1.919	1.88	1.457	1.535	30	0.078
72	15a	1.919	1.88	1.384	1.269	90	-0.115
73	15a	1.919	1.88	1.254	1.171	180	-0.083
74	16a	1.666	5.49	0.791	0.911	30	0.12
75	16a	1.666	5.49	0.151	0.454	90	0.303
76	7a	0.906	5.76	0.368	0.695	20	0.327

Row	Test #	G0 (mM)	P/G	Expt (mM)	G	Theo (mM)	G	Time (min)	Theo G- Expt G (mM)
77	7a	0.906	5.76	0.336		0.622		30	0.286
78	7a	0.906	5.76	0.19		0.47		60	0.28
79	7a	0.906	5.76	0.135		0.378		90	0.243
80	7a	0.906	5.76	0.104		0.317		120	0.213
81	7a	0.906	5.76	0.072		0.242		181	0.17
82	7a	1.666	3.49	1.129		1.14		30	0.011
83	7a	1.666	3.49	0.692		0.774		90	0.082
84	7a	1.666	3.49	0.446		0.604		180	0.158
85	7a	1.666	3.49	0.454		0.587		199	0.133
86	8a	1.666	10.9	0.215		0.478		30	0.263
87	OGCT	2.439	4.9	1.064		1.16		31	0.096
88	OGCT	2.439	4.9	0.543		0.764		60	0.221
89	OGCT	2.439	4.9	0.336		0.56		91	0.224
90	SMECT	1.932	5.6	0.902		0.93		32	0.028
91	SMECT	1.932	5.6	0.616		0.614		60	-0.002
92	SMECT	1.932	5.6	0.429		0.427		93	-0.002
93	SMECT	1.932	5.6	0.342		0.335		121	-0.007
94	SMECT	1.932	5.6	0.219		0.225		182	0.006
95		1.666	9.72	0.372		0.55		30	0.178

*Time for Theoretical Max G (mM) is to within  $\pm 30$  seconds of Experimental Time*